



## Research Article

# Design, Environmental Validation, and Candidate Crop Screening in a Modular Micro-Lunar Greenhouse System under CELSS-Like Conditions

Tao Wei <sup>a,b</sup> • Olha Bakumenko <sup>b,\*</sup> • Yunfan Zhang <sup>c</sup>

<sup>a</sup>School of Business, Shandong Agriculture and Engineering University, Jinan, China | <sup>b</sup>Faculty of Agrotechnologies and Natural Resources Management, Sumy National Agrarian University, Sumy Region, Ukraine | <sup>c</sup>School of Bioagricultural Sciences, Nagoya University, Nagoya, Japan

## ABSTRACT

Controlled Ecological Life Support Systems (CELSS) require reliable in situ crop production for long-duration lunar and planetary habitation. However, existing research infrastructure remains divided between large, expensive facilities and conventional growth chambers that lack the environmental realism needed for standardized crop screening. This study aimed to design, engineer, and experimentally validate a Micro-Lunar Greenhouse System (MLGS) as a mid-scale modular platform for evaluating functionally diverse candidate crops under CELSS-like conditions. The 1.52 m<sup>3</sup> MLGS integrated automated control of atmospheric composition, temperature, relative humidity, airflow, hydroponics, and programmable LED lighting across three independent cultivation zones. *Mesembryanthemum crystallinum*, *Anredera cordifolia*, and *Anoectochilus roxburghii* were cultivated for 180 days under species-optimized MLGS conditions and compared with standard laboratory chamber conditions using three biological replicates per treatment. Platform performance and crop responses were assessed through environmental stability, growth, photosynthetic traits, nutritional and bioactive composition, resource-use efficiency, waste-processing capacity, and microbial safety. The MLGS maintained environmental setpoints within  $\pm 0.8^{\circ}\text{C}$ ,  $\pm 1.5\%$  relative humidity, and 25–35 ppm CO<sub>2</sub> of target values for more than 97% of operating time, with low spatial heterogeneity among cultivation zones. Relative to the control, the optimized MLGS treatment increased biomass by 38–62%, enhanced key nutritional or bioactive compounds by 24–46%, and improved water-use efficiency by 25–55%. Nitrogen and phosphorus removal from simulated waste streams reached 58–79% and 47–70%, respectively, and no foodborne pathogens were detected. These results validate the MLGS as a reproducible bridge platform between large CELSS facilities and conventional growth chambers, supporting standardized crop screening for future space agriculture applications.

**KEYWORDS** climate-resilient agriculture • environmental control • food security • ground simulation • resource efficiency • space agriculture • sustainable agriculture

## ARTICLE CITATION

T. Wei, O. Bakumenko, Y. Zhang, "Design, Environmental Validation, and Candidate Crop Screening in a Modular Micro-Lunar Greenhouse System under CELSS-Like Conditions," International Journal of Environment, Engineering and Education, Vol. 8, No. 2, pp. 175–205, 2026. <https://doi.org/10.55151/ijeedu.v8i2.452>

## \*CORRESPONDENCE

Olha Bakumenko  [lady.bakumenko88@gmail.com](mailto:lady.bakumenko88@gmail.com)  Department of Plant Protection, Faculty of Agrotechnologies and Natural Resources Management, Sumy National Agrarian University, 160 Herasyma Kondratieva Street, Sumy, 40000, Ukraine  <https://orcid.org/0000-0003-1625-7401>



Copyright © 2026 by the author(s). Licensed by Three E Science Institute (International Journal of Environment, Engineering and Education). This is an open-access article distributed under the terms of the [Creative Commons Attribution-ShareAlike 4.0 \(CC BY-SA\)](https://creativecommons.org/licenses/by-sa/4.0/) International License which permits unrestricted use, distribution, and reproduction in any medium, provided the original work is properly cited and any derivative works are distributed under the same license.

## 1. INTRODUCTION

Long-duration human exploration of the Moon and Mars will require far more than incremental improvements in storage, packaging, and resupply logistics. As missions become longer, more distant, and more operationally autonomous, the continuous transport of food and life-support consumables from Earth becomes increasingly constrained by launch mass, mission architecture, cost, risk, and system vulnerability [1]–[3]. For this reason, bioregenerative life support systems (BLSS), often discussed within the broader controlled ecological life support systems (CELSS) framework, are now widely recognized as a strategic requirement for sustained extraterrestrial habitation rather than a speculative add-on to physicochemical life-support technologies [4], [5]. As De Micco et al. [6] emphasized, long-term space exploration will increasingly depend on life-support systems capable of producing and recycling critical resources within closed environments. More recently, Porterfield et al. [7] argued that logistical burden, technology limits, and health-and-safety risks together make current resupply-dependent approaches insufficient for future endurance-class lunar habitation.

Within BLSS/CELSS architectures, plants occupy a uniquely multifunctional role. They do not merely provide edible biomass; they also support oxygen regeneration, carbon dioxide removal, water recovery through transpiration, and the biological integration of waste-recycling loops. Wright et al. [8] further argued that space-controlled environment agriculture should be understood as an intrinsically circular and resource-efficient design paradigm, one that can inform both extraterrestrial habitation and next-generation terrestrial controlled-environment agriculture. This systems perspective is especially important because future space crop production must support not only caloric supply, but also nutritional adequacy, sensory acceptability, dietary diversity, and crew behavioral health. In that context, NASA's recent space-crop roadmap has stressed that crop suitability for exploration missions cannot be judged by productivity alone; it must also be evaluated through a structured Crop Readiness Level (CRL) framework that includes morphology, safety, nutrient content, processing suitability, and mission relevance [9], [10].

However, translating terrestrial controlled-environment cultivation into a mission-relevant CELSS platform remains a substantial systems-engineering challenge. In modern greenhouses, environmental control already requires the coordinated regulation of temperature, humidity, light, and CO<sub>2</sub> rather than single-factor optimization [11], [12]. In closed habitats, that challenge becomes more complex because these variables interact dynamically with canopy gas exchange, nutrient delivery, water balance, system sanitation, and microbial ecology. Elevated CO<sub>2</sub>, for example, may enhance photosynthetic carbon assimilation and improve yield or some quality traits under certain cultivation

conditions, but its effects remain crop-specific and context-dependent [13], [14]. Likewise, high air humidity does not merely alter transpiration; it can also suppress salicylic-acid-mediated defense responses and thereby increase disease susceptibility [15], [16]. At the same time, the plant microbiome is increasingly recognized as a major determinant of crop productivity, resilience, and biosafety, meaning that crop evaluation under CELSS-like conditions should include microbial stability and ecological compatibility rather than biomass output alone [17], [18].

Another critical but often underappreciated issue is that control fidelity is not equivalent to set-point control alone. A cultivation system may report acceptable nominal values for temperature, CO<sub>2</sub>, or humidity, while still producing biologically meaningful gradients in airflow, boundary-layer conditions, or spatial microclimate. Peiro et al. [19], working in the MELiSSA Higher Plant Chamber, showed that inadequate air distribution caused uneven lettuce growth in an otherwise highly controlled closed chamber, and that improved airflow design substantially enhanced crop uniformity. This finding is highly relevant for CELSS-oriented crop screening because it shows that platform quality must be evaluated in terms of stability, uniformity, and repeatability, not simply whether individual sensors reach their target values. As a result, robust crop screening for space applications should assess growth, nutritional quality, resource-use efficiency, environmental resilience, and microbial safety under tightly controlled and spatially reliable conditions.

A second major barrier is methodological. Existing infrastructures for CELSS-related crop research remain polarized between very large integrated ecological testbeds and small chamber-scale cultivation systems. At one end, landmark facilities such as BIOS-3, CEEF, and Lunar Palace 1 have provided indispensable system-level evidence that closed ecological support can sustain long-duration human habitation and coupled material circulation. BIOS-3 was foundational in demonstrating early bioregenerative life-support concepts in a sealed environment [20]. CEEF integrated plant, animal, and human habitation modules and demonstrated coupled circulation of air, water, food, and waste streams across multiple biological subsystems [21]–[23]. Most recently, the Lunar Palace 365 mission demonstrated 370 days of high-closure operation in Lunar Palace 1, achieving full recycling of oxygen and water for human use and 98.2% overall closure for materials essential to human survival [24]. These facilities, however, are inherently large, operationally complex, and low-throughput, making them poorly suited to routine comparative screening of multiple candidate crops and cultivation recipes.

Advanced plant-growth chambers and controlled-environment platforms provide high precision and strong repeatability for mechanistic studies, but they often lack the coupled ecological realism and experimental

architecture needed for CELSS-oriented screening. Even sophisticated chamber systems such as the MELiSSA Higher Plant Chamber emphasize highly controlled hydroponic cultivation and atmospheric regulation, yet they are still not intended to replace integrated ecosystem-level testbeds [25]. This leaves an important experimental gap: researchers still lack a mid-scale, modular, multi-zone platform that combines the control fidelity of chamber systems with the ecological and operational relevance needed for standardized, repeated, long-duration screening of candidate space crops. This gap becomes especially important when screening non-conventional or functional crops whose value may lie not only in yield, but also in nutrient density, medicinal potential, stress tolerance, or compatibility with closed-loop waste and water management.

The significance of this gap is reinforced by current NASA crop-selection strategy. Fritsche et al. [9] noted

that only a limited number of crops are presently reliable enough for space-production efforts, and that future testing must move systematically from basic crop identification to cultivar screening, environmental validation, food safety, and mission integration through the CRL framework. Related NASA crop-testing efforts on microgreens have similarly shown that candidate crops for space systems must be evaluated under exploration-relevant conditions for yield, nutritional composition, microbiological baseline, and sensory acceptability, rather than only under standard laboratory growth conditions. These developments indicate that the field now needs not only better crops, but also better screening infrastructure—platforms that can reproduce CELSS-relevant environmental conditions with sufficient stability and throughput to generate reproducible, decision-grade data for crop selection.

**Table 1.** Comparison of representative CELSS and controlled-environment platforms by scale, control scope, multi-zone capability, and documented continuous operation.

Platform	Representative scale/volume	Key controlled variables / functions	Representative control fidelity	Multi-species / multi-zone capability	Maximum documented continuous operation
BIOS-3 [20]	Large historic closed habitat / 315 m <sup>3</sup>	Closed ecological support with crewed compartments and phytotrons	n.r. in open primary sources	Yes, but not equivalent to modern parallel crop-screening zones	180 days
CEEF [21], [26], [27]	Large integrated ecological facility / ≈1,025 m <sup>3</sup> across published core modules; 150 m <sup>2</sup> plant cultivation area	Plant cultivation, atmospheric exchange, human/animal/crop material circulation	n.r. in open primary sources	Yes	Up to 4 weeks documented closed habitation experiments; longer annual model-ecosystem duration was planned/reported separately; 120 days
Lunar Palace 1 [24], [28]	Large integrated BLSS analog / 500 m <sup>3</sup>	Plant production, water recovery, waste processing, long-duration closed operation	Environmental stability demonstrated, but unified accuracy figures not consistently reported in open source	Yes	370 days
Advanced closed plant chambers (MELiSSA HPC) [19]	Chamber scale / 9 m <sup>3</sup> in representative HPC	Tight control of temperature, RH, CO <sub>2</sub> , light, and hydroponics	Good chamber controllability and homogeneity reported; exact accuracy is model-dependent	Limited to moderate; usually chamber-specific rather than true multi-zone ecological screening	6–8 weeks per documented crop experiment
MLGS (this study)	1.52 m <sup>3</sup>	Temperature, RH, CO <sub>2</sub> , programmable light, airflow, nutrient delivery, real-time monitoring, independent zones	±0.8°C, ±1.5% RH, 25–35 ppm CO <sub>2</sub>	Yes (3 independent zones)	180 days (validated)

Note. T = temperature; RH = relative humidity; n.r. = not reliably reported in the primary/open technical sources checked.

To clarify the current infrastructure landscape, Table 1 positions representative CELSS and controlled-environment platforms across scale, control scope, methodological value, and suitability for routine crop

screening. The comparison highlights a recurring pattern: large integrated facilities offer high ecological realism but low throughput, whereas chamber-scale systems offer high controllability but limited ecosystem relevance. The

unresolved need, therefore, is for a bridge platform that is sufficiently compact for repeated experimentation, sufficiently precise for long-duration environmental control, and sufficiently flexible for multispecies crop screening under CELSS-like conditions [29], [30].

In response to this need, the present study develops and validates the Micro-Lunar Greenhouse System (MLGS) as a compact, modular, CELSS-oriented crop-screening platform. The purpose of MLGS is not to replace full BLSS demonstrators such as Lunar Palace 1, but to function as an experimental bridge between simplified plant-growth chambers and large integrated closed-ecosystem facilities. Specifically, the platform is designed to provide autonomous multi-parameter control of temperature, relative humidity, CO<sub>2</sub> concentration, airflow, nutrient delivery, and programmable spectral lighting across independent cultivation zones, while also supporting real-time environmental monitoring and repeated long-duration operation. The central hypothesis of this study is that a mid-scale, tightly controlled greenhouse platform can maintain CELSS-relevant environmental conditions with sufficient stability and spatial uniformity to support reproducible multispecies screening, and that candidate crops grown under species-optimized CELSS-like recipes can be differentiated not only by growth, but also by nutritional quality, resource-use efficiency, waste-processing relevance, and microbial safety.

Accordingly, the objectives of this study are: (i) to design and engineer an MLGS platform capable of autonomous multi-parameter control across independent cultivation zones; (ii) to validate environmental stability, spatial uniformity, and operational consistency during 180 days of continuous operation; (iii) to establish a

standardized screening framework for candidate CELSS crops and cultivation recipes; (iv) to demonstrate that framework using *Mesembryanthemum crystallinum*, *Anredera cordifolia*, and *Anoectochilus roxburghii* as contrasting functional crop types; and (v) to quantify crop performance in terms of growth, nutritional quality, resource-use efficiency, waste-processing relevance, and microbial safety. Through these objectives, the study positions MLGS as a methodological contribution to space-agriculture research, with novelty centered on standardized, reproducible crop screening under CELSS-like conditions rather than on platform scale alone.

## 2. LITERATURE REVIEW

### 2.1. Conceptual Framework

This review is organized around a conceptual framework (Figure 1) that illustrates the hypothesized relationships among MLGS design features, environmental control outcomes, plant physiological responses, and CELSS suitability metrics. Each thematic section examines literature supporting these relationships and identifies the gaps that the MLGS is intended to address.

Figure 1 presents a sequential framework in which MLGS design features, such as modular structure, sensors, and control systems, promote environmental stability, which in turn regulates plant physiological responses. These responses then determine key CELSS suitability metrics, including biomass production, nutritional quality, and resource-use efficiency, ultimately informing evaluation of the selected candidate crops.

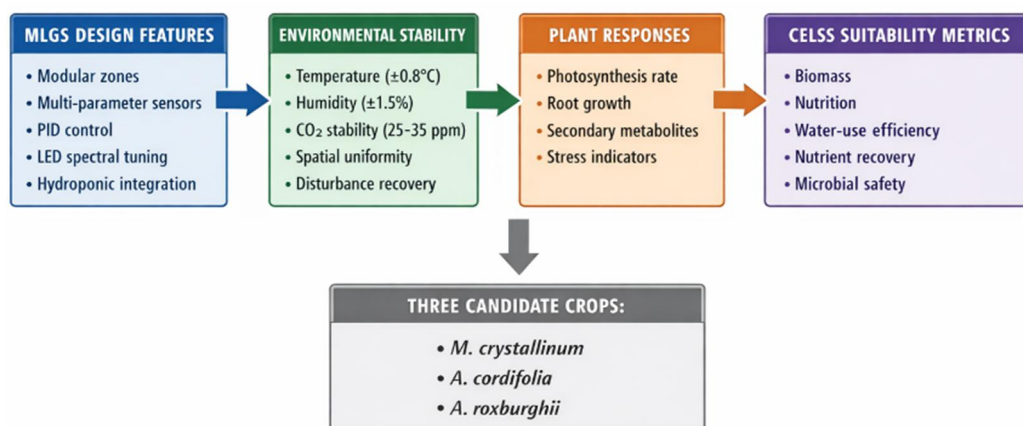


**Figure 1.** Conceptual framework linking MLGS design features, environmental control performance, plant physiological responses, and CELSS suitability metrics.

### 2.2. CELSS Operational Requirements and the Role of Plant Systems

Research on Controlled Ecological Life Support Systems (CELSS) has increasingly shown that integrated biological systems can support multi-year human space missions. Fu et al. [24], in their evaluation of the Lunar Palace 365 mission, demonstrated that closed ecosystems

incorporating humans, plants, and microorganisms can maintain continuous oxygen recycling and food production during extended isolation. Using Monte Carlo reliability analysis, Hu et al. [31] examined the same ecosystem and found that system stability depends strongly on crop productivity and subsystem redundancy. In Lunar Palace 1, Zhao et al. [28] described a water-

recycling system showing that integration of physicochemical purification and microbial treatment can effectively sustain water quality. Liu et al. [32] subsequently examined the architectural integration of crop cultivation modules in Chinese lunar base planning and emphasized their dual roles in atmospheric regeneration and food supply. Porterfield et al. [7] summarized global investment in bioregenerative life-support research and concluded that plant-based approaches must continue to play a central role in sustainable lunar exploration.

Plant-microbe interactions in closed systems have also emerged as critical determinants of system resilience. De Micco et al. [6] showed that microbial symbiosis promotes nutrient cycling and ecosystem stability. However, Poulet et al. [10] identified persistent technical challenges in large-scale crop production for lunar and Martian missions, particularly with respect to productivity, resource-use efficiency, and environmental control.

Subsequent studies have increasingly focused on optimizing crop growth under space-relevant conditions. Morsi et al. [33] demonstrated that substrate structure and fertilizer formulation strongly influence both leaf yield and mineral composition in mizuna grown under simulated spaceflight conditions. Research on Brassica rapa cultivars highlighted their nutritional value while also identifying long-term productivity constraints [34]. Analyses of microbial communities further showed that light conditions during tomato cultivation on the ISS altered rhizosphere microbial composition and, consequently, plant health [35]. Studies on microgravity-adapted fertilizers likewise reported improved efficiency of nutrient delivery systems for space crops [36].

Flight experiments have continued to validate the feasibility of space crop production while also clarifying the remaining challenges. Buncek et al., (2024) showed that “pick-and-eat” leafy crops can provide fresh food during missions, although production capacity remained limited [37]. Wheeler et al. [38] investigated CO<sub>2</sub> conditions and found high photosynthetic rates under moderate CO<sub>2</sub> concentrations, but substantial stress at elevated levels. Burgess et al. [39] demonstrated that biofortification under controlled conditions increased vitamin and antioxidant concentrations in lettuce. Hasenstein et al. [40], [41] reported transcriptional and metabolomic changes in radish grown in space. Khodadad et al. [10] characterized microbial communities associated with peppers cultivated on the ISS and identified implications for food safety. Maffei et al. [42] reproduced plant physiological responses to space conditions, whereas Fountain et al. [43] emphasized the increasingly central role of plant science in space exploration. Ortega-Hernandez et al. [44] concluded that future CELSS crops should exhibit compact growth, high photosynthetic efficiency, and compatibility with hydroponic cultivation.

Collectively, this literature indicates that CELSS crop production must simultaneously satisfy several criteria, including stable biomass production, nutrient recycling capacity, microbial community control, and nutritional value. Nevertheless, existing studies have largely relied either on large integrated platforms [24], [32] or on small growth chambers [33], [41]. Intermediate-scale platforms capable of systematic plant screening under coupled CELSS-like conditions remain largely absent.

### 2.3. Limitations of Existing Large-Scale and Small-Scale Experimental Platforms

Current CELSS crop research is structured around two broad experimental platform types, each with distinct strengths and limitations. Large integrated systems such as Lunar Palace-1 [24], [31], CEEF [1], and BIOS-3 [2] function as full-service life-support simulators that enable long-duration, system-level investigations. These facilities have generated foundational knowledge on closed ecological systems. However, they are capital intensive, operationally complex, and limited in experimental throughput, making them impractical for screening large numbers of crop candidates.

At the other end of the spectrum, conventional growth chambers provide relatively low-cost, high-throughput controlled environments. However, they generally lack the coupled environmental control characteristic of closed systems. Most commercial units cannot simultaneously regulate CO<sub>2</sub> concentration, humidity, airflow, and spectral light with the precision required for accurate CELSS simulation [22], [32]. In addition, they often lack integrated monitoring systems for assessing long-term operational stability.

Ground-based simulation technologies have improved substantially in recent years. Automated closed hydroponic systems have been shown to enhance sustainability, although sensor reliability remains problematic [45]. Sustainability analyses of vertical farming have highlighted its high energy demand [46]. Experiments involving closed water systems have demonstrated that microbial processes play a central role in system stability [47]. More broadly, syntheses of bioregenerative life-support systems have concluded that integrated biological processes are essential for life-support stabilization [48].

Environmental simulation studies have also investigated specific stressors relevant to space agriculture. A comparison of lettuce growth under low and high atmospheric pressure found only limited effects on growth [49]. Studies of microgravity effects on plants indicated altered auxin regulation [50]. Fahrion et al. [51] evaluated cyanobacterial bioreactor cultivation and showed that these systems can produce oxygen, although uncertainties regarding scalability remain. Molecular studies revealed novel Arabidopsis phenotypes under microgravity [52] as well as shared transcriptional responses across multiple spaceflight experiments [53],

[54]. Haveman et al. [55] further improved automated nucleic acid extraction as a tool for in situ plant health monitoring.

**Table 2.** Literature synthesis: Comparison of key CELSS crop studies by platform type.

Study	Platform Type	Species	Parameters Controlled	Duration	Key Metrics / Research Focus	Main Limitation
Fu et al. [24]	Lunar Palace-1 (500 m <sup>3</sup> )	Multiple crops	Temperature, RH, CO <sub>2</sub> , light, nutrient solution	365 days	System closure, O <sub>2</sub> recycling, long-term ecosystem operation	High infrastructure cost and low experimental throughput limit its utility for rapid crop screening
Hu et al. [31]	Lunar Palace-1	Multiple crops	As above	370 days	Reliability and subsystem redundancy analysis	Focused on retrospective reliability assessment rather than prospective crop-platform experimentation
Zhao et al. [28]	Lunar Palace-1	Multiple crops	Water quality and recycling processes	370 days	Water recovery and subsystem integration	Addresses a specific subsystem rather than whole-platform crop evaluation
Morsi et al. [33]	Growth chamber	Mizuna	Temperature, RH, light	28 days	Leaf yield and mineral composition	Lacked coupled CO <sub>2</sub> control and full CELSS-like environmental integration
Darby et al. [34]	Growth chamber	<i>Brassica rapa</i>	Standard chamber conditions	60 days	Nutritional potential	Useful for crop characterization, but not for integrated CELSS simulation
Spern et al. [35]	ISS Veggie	Tomato	ISS ambient environment with LED lighting	64 days	Rhizosphere microbiome and plant health	Limited control over CO <sub>2</sub> and humidity constrained environmental reproducibility
Bunchek et al. [37]	ISS	Leafy greens	ISS ambient conditions	Multiple harvest cycles	Edible biomass production	Demonstrated feasibility, but production scale remained limited
Wheeler et al. [38]	Growth chamber	Salad crops	Temperature, RH, CO <sub>2</sub>	56 days	Photosynthetic response and growth performance	Evaluated a narrow crop set under partially coupled conditions
Hasenstein et al. [40], [41]	ISS + ground comparison	Radish	ISS ambient environment	27–56 days	Gene expression and metabolic response	Uncontrolled environmental variation reduced interpretability for platform validation
Khodadad et al. [56]	ISS	Chile peppers	ISS cultivation environment	137 days	Microbial community structure	Primarily descriptive; did not provide integrated platform-performance validation
Cossu et al. [45]	Automated hydroponic system	Leafy greens	Temperature, RH, nutrient management	60 days	Sustainability and automation performance	Did not include full atmospheric coupling, especially CO <sub>2</sub> regulation
Stutte et al. [49]	Hypobaric chamber	Lettuce	Pressure, temperature, RH	21–35 days	Growth response under reduced pressure	Examined a single environmental stressor rather than a coupled cultivation environment
MLGS (this study)	Mid-scale modular platform (1.52 m <sup>3</sup> )	Three functional crop types	Temperature, RH, CO <sub>2</sub> , light spectrum, airflow, nutrient management (fully coupled)	180 days	Biomass, nutritional quality, water-use efficiency, microbial safety, resource recovery, and control stability	Designed to address the gap between high-realism/low-throughput systems and high-throughput/low-coupling chambers

Existing CELSS crop research platforms remain divided between large integrated systems that offer high ecological realism but limited throughput, and smaller chamber-based systems that support controlled experimentation but lack fully coupled environmental regulation. No previous platform has combined a mid-scale footprint, long-duration operation, coupled multi-parameter control, and multispecies evaluation within a single framework. The MLGS was designed specifically to address this methodological gap.

#### 2.4. Environmental Control Architecture and Sensor/Control Performance

Accurate environmental management is fundamental to reproducible CELSS crop research. Recent advances in controlled-environment agriculture have shown that stable cultivation conditions can be achieved through integrated sensor networks, automated actuation, and closed-loop control systems that regulate temperature, relative humidity, CO<sub>2</sub> concentration, light environment, and root-zone conditions in real time [29], [57], [58]. Reviews of controlled-environment systems further indicate that control precision directly influences crop productivity, resource-use efficiency, and overall system performance, while life-cycle assessments highlight the energy implications of precision control in comparison with conventional production systems [59], [60]. Contemporary research-grade platforms therefore rely on distributed sensing, digital communication, and calibrated lighting and gas-monitoring systems to support reliable multi-parameter regulation.

Control strategies have also evolved beyond simple on-off regulation toward more advanced multivariable approaches, including PI/PID-based control, adaptive tuning, and decoupling methods designed to manage the nonlinear and coupled dynamics of plant-growth environments [58], [61]. In this context, performance can no longer be assessed by setpoint tracking alone; disturbance rejection, spatial uniformity, actuator robustness, and long-term stability are equally important, particularly under dynamic plant loads created by transpiration, equipment cycling, and routine sampling. Space-based validation studies, such as those conducted with the Advanced Plant Habitat on the International Space Station, further demonstrate that high-fidelity crop experiments depend on tightly integrated control of light, humidity, CO<sub>2</sub>, temperature, photoperiod, and root-zone moisture [62].

Despite these advances, long-duration validation remains insufficiently reported in the literature. Many

studies demonstrate initial control capability or short-term performance, but far fewer assess sustained multi-parameter stability under active cultivation over extended periods. This limitation is especially significant for CELSS applications, where systems must remain stable for months or years with minimal external intervention [55]. Although individual sensing and control technologies are now well established, published studies rarely provide robust validation of long-term control stability, disturbance recovery, and spatial uniformity under dynamic plant loads. The MLGS addresses this gap by evaluating continuous multi-parameter control over 180 days of active crop cultivation.

#### 2.5. Candidate Crop Traits for CELSS and Species

Selecting crop species for CELSS requires consideration of multiple functional characteristics beyond yield potential alone. Ortega-Hernandez et al. [44] identified compact growth habit, photosynthetic efficiency, and hydroponic compatibility as critical criteria. In addition, nutritional diversity, stress tolerance, and suitability for closed-loop resource recycling are increasingly important in candidate crop selection. The three species selected for this study represent complementary functional types with distinct potential contributions to future CELSS crop portfolios.

*Mesembryanthemum crystallinum* (common ice plant) is a halophytic succulent valued both as a vegetable crop and as a model species in stress physiology research. As a facultative CAM plant, it can shift its photosynthetic pathway under environmental stress, a trait that may be advantageous in variable space habitats. Its epidermal bladder cells are associated with sodium accumulation, suggesting potential utility in bioregenerative salinity management. Nutritional analyses have also indicated a favorable mineral composition, particularly with respect to potassium and calcium [33].

*Anredera cordifolia* (Madeira vine) is a protein-rich herbaceous perennial vine with potential as a continuous-harvest vegetable. Its tuberous roots may support repeated harvest within a single biomass cycle and thereby enhance food production per unit area [37]. Its adaptability to trellis-based vertical cultivation may also support efficient use of limited production space.

*Anoectochilus roxburghii* (jewel orchid) is a medicinal understory plant with potential for producing high-value bioactive compounds within CELSS. Li et al. [63] characterized its functional food potential and reported antioxidant-related compounds, including polysaccharides, flavonoids, and alkaloids. .

**Table 3.** Functional traits and CELSS-relevant characteristics of the selected candidate species.

Species	Functional Type	Key CELSS-Relevant Traits	Complementary Role	Literature Support
<i>Mesembryanthemum crystallinum</i>	Halophytic leafy vegetable	Salt accumulation (bladder cells), facultative CAM, high K/Ca, responsive to CO <sub>2</sub> enrichment	Salinity management, mineral supplementation	Morsi et al., [33]

Species	Functional Type	Key CELSS-Relevant Traits	Complementary Role	Literature Support
<i>Anredera cordifolia</i>	Protein-rich vine vegetable	High protein (>20% DW), continuous harvest, rapid biomass, vertical growth	Dietary protein, space-efficient production	Bunchek et al., [37]
<i>Anoectochilus roxburghii</i>	Medicinal understory plant	Bioactive compounds (polysaccharides, flavonoids), shade tolerance, low light requirement	High-value phytochemicals, multi-tier cultivation	Ortega-Hernandez et al., [44]; Li et al., [63]

These three species represent complementary functional niches relevant to CELSS crop portfolios, namely stress-tolerant edible biomass (*M. crystallinum*), vertically deployable edible vine biomass (*A. cordifolia*), and high-value medicinal phytochemical production (*A. roxburghii*). While each species has been studied individually, no previous study has evaluated this functionally diverse set under identical controlled conditions with CELSS-relevant environmental parameters and resource-use metrics. The MLGS enables systematic comparison across functional types using standardized protocols.

## 2.6. Evaluation Metrics for Platform Validation

Comprehensive platform validation requires assessment across multiple dimensions, including environmental control stability, crop productivity, nutritional quality, resource-use efficiency, and microbial safety. Recent BLSS and crop-readiness frameworks indicate that candidate evaluation should extend beyond biomass alone to include nutritional value, operational performance, and food safety under controlled cultivation conditions [64]–[66].

Environmental control stability metrics include setpoint tracking accuracy, typically expressed as mean absolute error and standard deviation; spatial uniformity, commonly represented by the coefficient of variation; disturbance recovery time; and long-term drift. These metrics are essential because reproducible crop experiments depend on sustained regulation of temperature, relative humidity, CO<sub>2</sub> concentration, light environment, and root-zone conditions over extended cultivation periods. Evidence from controlled plant-growth platforms and recent greenhouse control studies further shows that performance under coupled climatic variables, actuator interactions, and operational disturbances is central to assessing platform reliability [61], [62], [67].

Crop productivity metrics should extend beyond total biomass to include harvest index, growth rate, phenological timing, and yield per unit area, all of which are necessary for comparing space-use efficiency among crop candidates. In the context of space farming, productivity must be interpreted not only in terms of mass accumulation, but also in relation to crop architecture, harvestable fraction, and operational suitability within constrained cultivation volumes [10], [37], [64], [65].

Nutritional quality assessment must address both universal nutritional parameters and species-specific functional compounds. Protein content, amino acid

balance, fatty acid composition, vitamins, minerals, and antioxidant-related metabolites are all directly relevant to crew health during long-duration missions. In addition, the possibility of targeted biofortification under controlled cultivation conditions has become increasingly important in space-crop research, particularly for leafy vegetables used as model crops [33], [39], [68].

Resource-use efficiency metrics are equally critical in closed-loop systems. Water-use efficiency affects recycling demand, CO<sub>2</sub> fixation efficiency influences atmospheric management, and nutrient recovery potential determines the extent to which crop production can be integrated with waste-processing streams. Recent hydroponic and nutrient-recovery studies have underscored that precise nutrient-solution management is indispensable for improving both nutrient-use efficiency and water-use efficiency, while also highlighting the technical challenges associated with recovering hydroponically relevant nutrient forms from waste streams [28], [38], [69], [70].

Microbial safety has emerged as an essential validation dimension following ISS cultivation experiments showing that crop production conditions influence both microbial load and microbial community structure. Accordingly, total culturable counts, pathogen screening, and rhizosphere or phyllosphere community profiling provide important indicators of both food safety and system health. These considerations are also consistent with crop-readiness frameworks, which explicitly include food safety as part of space-crop qualification [65], [68].

Previous studies have evaluated subsets of these dimensions, but the literature still rarely reports integrated validation across environmental stability, productivity, nutrition, resource efficiency, and microbial safety for functionally diverse species under coupled CELSS-like conditions and long-duration operation. The MLGS experimental protocol was therefore designed to address this multidimensional assessment gap.

## 2.7. Literature Synthesis and Research Gap Summary

The Micro-Lunar Greenhouse System (MLGS) was designed specifically to address this integrated gap by providing a mid-scale, multi-parameter-controlled platform capable of long-duration, multispecies cultivation with comprehensive monitoring across all five metric domains. The conceptual framework shown in Figure 1 therefore guides both the experimental design and the interpretation presented in the following sections.

The literature reviewed across these themes leads to five main conclusions.

- CELSS crop production must satisfy multiple simultaneous requirements, including biomass production, nutritional value, resource recovery, and microbial safety; these requirements cannot be evaluated on the basis of yield alone [24], [44], [66].
- Existing research platforms remain strongly polarized. Large integrated BLSS facilities provide high system realism but limited experimental throughput, whereas conventional chambers and flight hardware support faster or more targeted experimentation but often lack fully coupled environmental control or broad screening capacity [33], [45], [55], [62], [64].
- Technologies for multi-parameter environmental regulation are available, but robust long-duration validation under dynamic plant loads remains limited in the published literature. In particular, relatively few studies report sustained performance in terms of disturbance rejection, coupled temperature–humidity control, data quality robustness, and long-term control stability during active cultivation [61], [62], [67].
- Functionally diverse crop candidates with complementary roles have not yet been systematically compared under standardized CELSS-like conditions. Current crop-selection frameworks emphasize not only productivity, but also nutritional contribution, food safety, and progression across increasingly space-relevant test environments [33], [44], [55], [65].
- Multidimensional validation remains insufficiently integrated. Although individual studies have addressed nutritional quality, microbial safety, environmental control, or resource efficiency, these dimensions are still seldom evaluated together within a single long-duration, multispecies platform study [38], [39], [68], [69].

### 3. MATERIALS AND METHODS

#### 3.1. System Design and Engineering

The design of the Micro-Lunar Greenhouse System (MLGS) was intended to meet four major technical goals: (1) accurate simulation of core CELSS environmental conditions, including temperature, humidity, CO<sub>2</sub>, and lighting, with precision comparable to large-scale systems; (2) a modular design allowing multiple crop species with different requirements to be cultivated simultaneously; (3) a small footprint and substantially lower cost compared with existing simulation platforms; and (4) extensive data capture to enable quantitative analysis of plant growth, harvest outcomes, and environmental correlations.

The system specifications were developed based on CELSS operational requirements and crop physiological tolerances [71]. The target environmental parameters

included a temperature range of 5–40°C with ±1°C regulation accuracy, relative humidity of 35–90% with ±2 percent accuracy, CO<sub>2</sub> concentration of 25–5000 μmol·mol<sup>-1</sup>, photosynthetic photon flux density of 0–3000 μmol·m<sup>-2</sup>·s<sup>-1</sup> with controllable spectral composition (400–750 nm), and air flow velocity of 0.1–1.0 m·s<sup>-1</sup> with ±0.1 m·s<sup>-1</sup> accuracy.

##### 3.1.1. Structural Design and Technical Specifications

The structural configuration of the MLGS was designed to maintain stable closed-environment conditions while ensuring hygienic operation, mechanical robustness, and effective environmental isolation. In closed and semi-closed plant production systems, environmental regulation depends not only on control hardware but also on the structural integrity and material selection of the cultivation chamber [72], [73]. Accordingly, the MLGS framework was constructed using 304 stainless steels, a material widely used in hygienic equipment because of its corrosion resistance, durability, and ease of cleaning under humid operating conditions [74]. The chamber had internal dimensions of 1.2 m × 0.8 m × 1.6 m, corresponding to a cultivation volume of 1.52 m<sup>3</sup>. This compact design represented an 85% reduction relative to CEEF and a 99% reduction relative to Lunar Palace-1, while reducing capital costs by more than 80% (see Suppl. Table S7).

The enclosure consisted of acrylic panels with a 20 mm insulating air gap and a 20 mm multi-layer structure (8 mm per layer), providing a thermal transmittance of 0.85 W·m<sup>-2</sup>·K<sup>-1</sup> and visible light transmittance of 92%. Such high-transmittance covering materials are important because enclosure optical and thermal properties directly affect light penetration, heat exchange, and microclimate stability in controlled-environment plant production [72]. Panel joints were sealed using food-grade silicone gaskets and aluminum compression frames, achieving an air leakage rate of less than 0.05 chamber volumes per hour at a pressure differential of 500 Pa. Additional access features included a 400 mm × 500 mm sealed operation door, four 100 mm sampling ports with silicone septum seals, and built-in observation windows with anti-condensation heating elements. Collectively, these features were intended to minimize uncontrolled exchange with the external environment and support precise environmental regulation for CELSS-oriented plant experiments [72], [73].

##### 3.1.2. Modular Architecture, Sensor Calibration, and Control Performance

The structural configuration of the MLGS was designed to maintain stable closed-environment conditions while ensuring hygienic operation, mechanical robustness, and effective environmental isolation. In closed and semi-closed plant production systems, environmental regulation depends not only on control hardware but also on the structural integrity and material selection of the

cultivation chamber, because temperature, humidity, gas composition, light, and air movement must be tightly controlled to support plant growth and system stability [72], [73]. Accordingly, the MLGS frame was constructed using 304 stainless steel, a material widely used in hygienic equipment due to its corrosion resistance, durability, and cleanability under humid operating conditions [74].

The chamber had internal dimensions of 1.2 m × 0.8 m × 1.6 m, corresponding to a cultivation volume of 1.52 m<sup>3</sup>, and this compact configuration represented an 85% reduction relative to CEEF and a 99% reduction relative to Lunar Palace-1 while reducing capital cost by more than 80% (see Suppl. Table S7). The enclosure consisted of acrylic panels with a 20 mm insulating air gap and a 20 mm multi-layer structure (8 mm per layer), providing a thermal transmittance of 0.85 W·m<sup>-2</sup>·K<sup>-1</sup> and visible light transmittance of 92%. Such high-transmittance enclosure materials are appropriate for controlled-environment plant production because the optical and thermal properties of covering materials directly influence light penetration, heat exchange, and microclimate stability [72], [75]. Panel joints were sealed with food-grade silicone gaskets and aluminum compression frames to minimize leakage, while a sealed operation door, sampling ports, and anti-condensation observation windows were incorporated to reduce uncontrolled exchange with the external environment and support precise CELSS-oriented environmental control [73].

The MLGS incorporated four functional modules—Environment Generation, Perception and Monitoring, Intelligent Control, and Crop Cultivation—reflecting the integrated control architecture commonly recommended for semi-closed plant production systems and smart greenhouse platforms [72], [76]. The Environment Generation Module regulated atmospheric, thermal, hydrological, and illumination conditions through proportional solenoid valves, NDIR CO<sub>2</sub> sensing,

thermoelectric cooling, ultrasonic humidification, regenerative dehumidification, and programmable LED arrays. This configuration is appropriate because greenhouse environmental control relies on coordinated regulation of CO<sub>2</sub>, temperature, humidity, and light, while programmable LEDs enable precise manipulation of spectral quality and intensity that directly affect photosynthesis, photomorphogenesis, and biomass production [72], [77]. The use of the Vaisala GMP252 is also technically consistent with this application, as the probe is designed for agriculture, greenhouses, and other demanding environments requiring stable CO<sub>2</sub> measurement [78].

The Perception and Monitoring Module employed distributed sensors with 10-minute sampling intervals, including NDIR CO<sub>2</sub> analyzers, SHT35 humidity sensors, PT100 temperature sensors, pH/EC electrodes, and dissolved oxygen optodes, which is consistent with the multi-sensor monitoring approach emphasized in recent smart greenhouse literature [76]. The Intelligent Control Module used a Siemens S7-1200 PLC implementing PID-based control with adaptive gain scheduling, a suitable choice because Siemens documents PID\_Compact for S7-1200/S7-1500 as a continuous PID controller with integrated optimization for process control [79]. The Crop Cultivation Module provided three independently controlled growing zones compatible with deep water culture, nutrient film technique, and aeroponics, which is relevant because these are among the most widely adopted soilless cultivation systems and differ in oxygenation, nutrient delivery, and crop-management characteristics [80]. Before each experimental cycle, sensors were calibrated against certified standards, and system performance was evaluated in terms of control stability rather than nominal sensor accuracy; this distinction is scientifically appropriate because steady-state CO<sub>2</sub> stability and recovery time better represent actual control performance than manufacturer accuracy alone [78], [81].

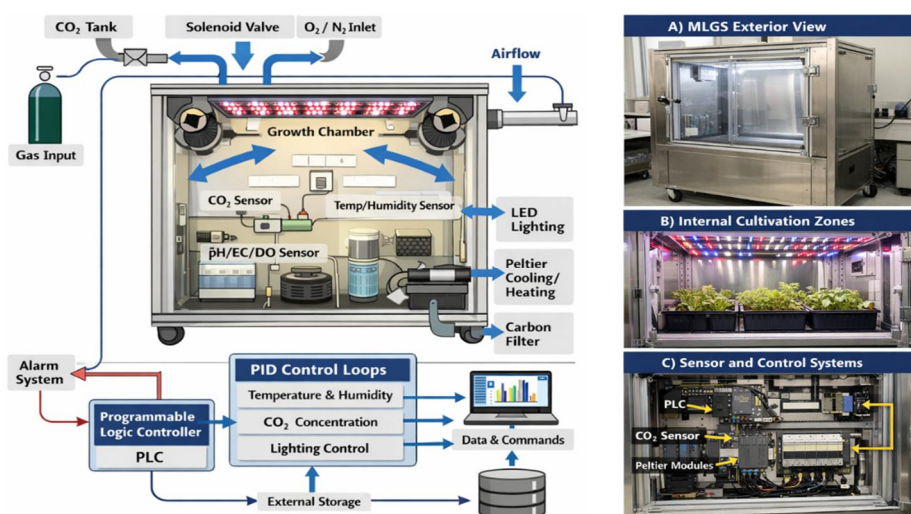


**Figure 2.** Micro-Lunar Greenhouse System (MLGS): (A) control architecture showing airflow, gas regulation, sensors, actuators, and PLC-based feedback loops; (B) physical implementation, including exterior view, cultivation chamber, and sensor/control subsystem.

Figure 2 illustrates the MLGS control architecture and system overview. The schematic shows airflow circulation, gas input and control components (CO<sub>2</sub> tank and solenoid valves), environmental sensors (CO<sub>2</sub>, temperature/humidity, pH/EC/DO), and actuators (LED lighting, Peltier modules, and carbon filtration). The programmable logic controller (PLC) coordinated PID-based control loops and recorded operational data. The right panel presents the external design, internal growth areas, and sensor/control subsystems.

### 3.2. Experimental Design and Crop Selection

This study compared two treatment packages: (1) the MLGS platform operated under species-specific optimized environmental conditions, and (2) standard laboratory growth conditions using a fixed environment for all species. Accordingly, the treatments differed in both cultivation platform and environmental regime. Therefore,

**Table 4.** Experimental treatment design comparing MLGS-optimized and standard laboratory control conditions across species, platform, and environmental parameters.

Treatment	Platform	Environmental Conditions	Species
MLGS-optimized	MLGS (1.52 m <sup>3</sup> )	Species-specific optimized (Tables 5-7)	Each species separately
Control	Growth chamber (Percival CU-36L5, 1.57 m <sup>3</sup> )	Fixed: 25±2°C, 70±5% RH, ambient CO <sub>2</sub> (~400 ppm), 200 μmol·m <sup>-2</sup> ·s <sup>-1</sup> light, 12 h photoperiod	All species

For each treatment, three independent biological replicates were conducted, with 20 homogeneous seedlings per species in each replicate (total n = 60 per treatment). Plants within each replicate were treated as subsamples, and replicate means were used for statistical analysis. To minimize spatial heterogeneity, plant positions were randomized weekly in both the MLGS cultivation zones and the control growth chamber [55]. The cultivation period lasted 6–10 months, encompassing full growth cycles for annual species and multiple harvests for perennial species.

A specific limitation applies to *Anoectochilus roxburghii*, for which the control light intensity (200 μmol·m<sup>-2</sup>·s<sup>-1</sup>) exceeded the reported optimal range for this understory species (50–150 μmol·m<sup>-2</sup>·s<sup>-1</sup>). This may have caused light stress in control plants and contributed to the large biomass difference observed, a point addressed further in the Discussion.

### 3.3. Cultivation Parameters and Environmental

Species-specific environmental regimes were established on the basis of preliminary optimization experiments and physiological tolerance ranges reported in the controlled-environment agriculture and space-crop literature. For *Mesembryanthemum crystallinum*, the optimized cultivation parameters included moderate day/night temperatures, relatively low humidity, elevated CO<sub>2</sub>, and deep-water hydroponic culture to support biomass accumulation and mineral enrichment; these parameters

all observed differences should be interpreted as the combined effect of MLGS hardware and environmental optimization, rather than the effect of the MLGS platform alone. All interpretations throughout this manuscript have been framed with this limitation in mind.

Three crop species were selected to represent complementary functions relevant to CELSS applications: *Mesembryanthemum crystallinum* as a halophytic leafy vegetable, *Anredera cordifolia* as a protein-rich vine vegetable, and *Anoectochilus roxburghii* as a medicinal understory plant. Selection was based on nutritional value, environmental adaptability, growth characteristics, and hydroponic suitability. Table 4 defines the two treatment groups used throughout the study: the MLGS platform under species-specific optimized conditions versus a standard laboratory growth chamber under fixed environmental settings, clarifying the confounded nature of the platform-plus-environment comparison.

are summarized in Table 5. In contrast, the cultivation regime for *Anredera cordifolia* was designed to reflect its thermophilic growth habit and rapid vegetative development, and therefore incorporated higher temperature and CO<sub>2</sub> setpoints, a longer photoperiod, and nutrient film technique cultivation to promote vine elongation and edible biomass production (Table 6). For *Anoectochilus roxburghii*, a shade-adapted medicinal understory species, the regime emphasized low-light and high-humidity conditions, together with aeroponic misting schedules and a modified Murashige and Skoog nutrient formulation, in order to support stable growth and bioactive compound accumulation under controlled conditions (Table 7).

**Table 5.** Optimized Parameters for *Mesembryanthemum crystallinum*

Parameter	Value
Temperature (day/night)	20–25°C / 15–18°C
Relative humidity	40–60%
CO <sub>2</sub> concentration	800–1200 μmol·mol <sup>-1</sup>
Airflow velocity	0.3–0.5 m·s <sup>-1</sup>
Light spectrum	Red:blue (3:1) + white
Light intensity	150–180 μmol·m <sup>-2</sup> ·s <sup>-1</sup>
Photoperiod	12–14 h
Cultivation method	Deep-water hydroponics
Nutrient solution pH	6.0–7.0

Parameter	Value
EC	800–1000 $\mu\text{S}\cdot\text{cm}^{-1}$ (seedling); 1200–1500 $\mu\text{S}\cdot\text{cm}^{-1}$ (growth)
Planting density	25 plants·m <sup>-2</sup>
Irrigation cycle	10 min circulation every 2 h

**Table 6.** Optimized Parameters for *Anredera cordifolia*

Parameter	Value
Temperature (day/night)	25–30°C / 20–22°C
Relative humidity	60–80%
CO <sub>2</sub> concentration	1000–1500 $\mu\text{mol}\cdot\text{mol}^{-1}$
Airflow velocity	0.2–0.3 m·s <sup>-1</sup>
Light spectrum	Full-spectrum white + 10–15% red
Light intensity	200–300 $\mu\text{mol}\cdot\text{m}^{-2}\cdot\text{s}^{-1}$
Photoperiod	14–16 h
Cultivation method	Nutrient film technique
Nutrient solution pH	6.0–6.5
EC	1000–1400 $\mu\text{S}\cdot\text{cm}^{-1}$
Planting density	25 plants·m <sup>-2</sup>
Irrigation cycle	15 min circulation every 3 h
Nutrient composition	N:P:K = 3:1:2

**Table 7.** Optimized Parameters for *Anoectochilus roxburghii*

Parameter	Value
Temperature (day/night)	23–25°C / 18–20°C
Relative humidity	70–85%
CO <sub>2</sub> concentration	600–800 $\mu\text{mol}\cdot\text{mol}^{-1}$
Airflow velocity	0.1–0.2 m·s <sup>-1</sup>
Light spectrum	Red:blue (7:3) + weak white
Light intensity	50–150 $\mu\text{mol}\cdot\text{m}^{-2}\cdot\text{s}^{-1}$
Photoperiod	10–12 h
Cultivation method	Aeroponic / mist culture
Nutrient solution pH	5.5–6.0
EC	500–800 $\mu\text{S}\cdot\text{cm}^{-1}$
Planting density	50 plants·m <sup>-2</sup>
Irrigation schedule	Mist 3–4 times daily (5–10 min each)
Nutrient formula	Modified MS ( <sup>1</sup> / <sub>4</sub> – <sup>1</sup> / <sub>2</sub> strength) + 0.1% humic acid

Note. Detailed physiological explanations and supporting references are provided in Table S1 – S3.

### 3.4. Measurement Variables and Analytical Procedures

#### 3.4.1. Growth and morphological traits

Plant height and crown width were measured weekly using digital calipers (Mitutoyo 500-196-30;  $\pm 0.01$  mm). Leaf area was determined biweekly with a leaf area meter (LI-3000C, LI-COR). At harvest, fresh and dry weights were recorded after enzyme deactivation at 105°C for 30 min, followed by drying at 75°C to constant weight. Root

morphological traits were assessed at 30-day intervals using WinRHIZO Pro 2019 to characterize root system development and architectural responses under the cultivation treatments.

#### 3.4.2. Physiological and biochemical analyses

Chlorophyll content was measured biweekly as SPAD values using a SPAD-502Plus chlorophyll meter (Konica Minolta). Gas-exchange parameters, including net photosynthetic rate (Pn), stomatal conductance (Gs), transpiration rate (Tr), and intercellular CO<sub>2</sub> concentration (Ci), were measured monthly using an LI-6800 portable photosynthesis system (LI-COR). Measurements were conducted between 09:00 and 11:00 h on five leaves per replicate, with three technical replicates per leaf, to reduce short-term environmental variation and improve analytical precision.

At harvest, nutritional quality was assessed using species-specific assays selected according to the major target metabolites of each crop. In *M. crystallinum*, sodium, potassium, and calcium concentrations were quantified by atomic absorption spectrophotometry (PerkinElmer PinAAcle 900T). In *A. cordifolia*, fatty acid composition was determined by gas chromatography (Agilent 7890B), and soluble protein content was quantified using the Coomassie blue method. In *A. roxburghii*, polysaccharide, flavonoid, and alkaloid contents were determined using the phenol-sulfuric acid, sodium nitrite-aluminum nitrate, and bromocresol green methods, respectively. In all species, vitamin C and soluble sugars were quantified by 2,6-dichloroindophenol titration and anthrone colorimetry, respectively [82]–[84].

#### 3.4.3. Microbial community analysis

Rhizosphere and phyllosphere samples were collected aseptically at harvest (n = 3 per treatment) for microbial community profiling. Total genomic DNA was extracted using the DNeasy PowerSoil Pro Kit (QIAGEN). The bacterial 16S rRNA gene V3–V4 region was amplified using primers 341F/805R, whereas the fungal ITS region was amplified using primers ITS1F/ITS2R. Amplicon libraries were sequenced on an Illumina MiSeq platform (2 × 300 bp). Raw sequence data were deposited in the NCBI Sequence Read Archive (SRA). Sequence processing and denoising were performed in QIIME2 2024.2 using DADA2, and taxonomic assignment was conducted against the SILVA 138.1 database for bacterial sequences and the UNITE v9.0 database for fungal sequences [85]–[87].

#### 3.4.4. Pathogen detection

To evaluate microbiological safety, targeted quantitative PCR (qPCR) assays were performed for *Salmonella* spp., *Escherichia coli* O157:H7, and *Listeria monocytogenes* using TaqMan chemistry. In parallel, culture-based enumeration was conducted on Plate Count Agar for bacteria and Potato Dextrose Agar for fungi to

complement molecular detection with cultivation-based estimates of microbial load.

#### 3.4.5. Resource-Use metrics

Water-use efficiency (WUE) was calculated as biomass accumulation divided by water consumption. Salt-use efficiency, evaluated only for *M. crystallinum*, was calculated as (crop salt absorption / nutrient solution salt content) × 100%. CO<sub>2</sub> fixation efficiency was determined by infrared gas analysis (LI-840A) based on chamber CO<sub>2</sub> depletion during the light period.

#### 3.4.6. Simulated waste degradation and nutrient recovery

Material-cycle efficiency was evaluated through two complementary approaches. First, crop residue degradation was quantified as gravimetric mass loss over 30 days. Second, degradation of the simulated waste liquid was monitored by high-performance liquid chromatography (HPLC; Agilent 1260 Infinity II). Nitrogen cycling was determined by Kjeldahl digestion, whereas phosphorus concentration was measured by molybdenum-antimony colorimetry at 700 nm.

Table 8 summarizes the composition of the synthetic waste liquid used to evaluate crop-based nutrient recovery, including the concentrations of urea, creatinine, uric acid, major electrolytes, and phosphate within a physiologically relevant pH range.

**Table 8.** Simulated astronaut waste liquid composition

Component	Concentration	Function
Urea	1.5 g·L <sup>-1</sup>	Primary nitrogen source
Creatinine	0.15 g·L <sup>-1</sup>	Nitrogenous waste marker
Uric acid	0.05 g·L <sup>-1</sup>	Purine metabolism product
Sodium chloride	5.0 g·L <sup>-1</sup>	Electrolyte balance
Potassium chloride	1.0 g·L <sup>-1</sup>	Potassium source
Potassium dihydrogen phosphate	0.5 g·L <sup>-1</sup>	Phosphorus and potassium source
pH	7.0–7.5	Physiological range

**Table 9.** Statistical models and analytical approaches applied to different outcome variable types in the experimental dataset

Outcome Type	Statistical Approach
Continuous variables (biomass, photosynthetic rate, etc.)	Linear mixed models with treatment as a fixed effect and replicate as a random effect; alternatively, one-way ANOVA on replicate means with cautious interpretation (n = 3)
Longitudinal data (weekly/monthly measurements)	Linear mixed models with repeated measures, including the time × treatment interaction
Establishment success (%)	Binomial generalized linear model (logistic regression)
Microbial counts (CFU)	Log-transformed count models
Pathogen detection (presence/absence)	Fisher's exact test
Diversity indices (Shannon, Chao1)	PERMANOVA (Bray-Curtis)

### 3.5. Statistical Analysis

#### 3.5.1. Experimental Unit and Replication

The experimental unit for statistical inference was the cultivation run (biological replicate). Plants within each run (20 per species) were treated as subsamples. All plant-level measurements were averaged to obtain replicate means (n = 3 per treatment) before inferential analysis, thereby avoiding pseudo replication.

#### 3.5.2. Sample Size Justification

Preliminary data (Cohen's d = 0.9, α = 0.05, power = 0.90) indicated a minimum requirement of 15 plants per group. To account for mortality and destructive sampling, 20 plants were included per replicate, resulting in three biological replicates per treatment. Thus, the total sample size was n = 60 plants per treatment for descriptive

purposes, whereas the inferential sample size remained n = 3.

#### 3.5.3. Statistical Models

Statistical models were selected according to outcome type to ensure consistency, transparency, and reproducibility across the multi-parameter dataset. Table 9 summarizes the analytical approaches applied to each response category.

#### 3.5.4. Assumption Testing and Multiple-Comparison Correction

Normality was assessed using the Shapiro-Wilk test, and homogeneity of variances was evaluated using Levene's test. When multiple comparisons were performed, p-values were adjusted using the Benjamini-Hochberg false discovery rate procedure [88].

### 3.5.5. Effect Size Estimation

Effect size was estimated using Cohen's  $d$ , calculated as:

$$d = \frac{|M_1 - M_2|}{SD_{pooled}} \quad (1)$$

where  $M_1$  and  $M_2$  are the means of the two groups, and interpreted as follows: 0.2, small; 0.5, medium; and 0.8, large [89]–[91].

### 3.5.6. Software and Data Presentation

All analyses were performed using SPSS v26.0 (IBM) and R version 4.2.1, with the lme4 package used for mixed-effects modeling. Results are presented as mean  $\pm$  SD from three biological replicates unless otherwise indicated. Statistical significance was defined as  $p < 0.05$ , and high significance was defined as  $p < 0.01$ .

## 4. RESULTS

### 4.1. MLGS System Performance Validation

Over the 180-day cultivation period, the MLGS sustained stable programmed environmental conditions, with all critical variables remaining within predefined operating limits for more than 97% of total operating time, indicating robust long-term system performance. Table 10 shows that control accuracy across all monitored parameters—temperature, relative humidity,  $\text{CO}_2$  concentration, airflow velocity, light intensity, root-zone temperature, pH, and EC—ranged from 97.6% to 100%. Disturbance recovery was rapid for actively controlled aerial variables, averaging  $12.1 \pm 2.3$  min for temperature,  $6.8 \pm 1.1$  min for relative humidity,  $8.3 \pm 1.4$  min for  $\text{CO}_2$ , and  $3.2 \pm 0.8$  min for airflow velocity. Spatial heterogeneity within cultivation zones was minimal, as reflected by low coefficients of variation for temperature (2.3%), relative humidity (3.1%),  $\text{CO}_2$  concentration (1.8%), and light intensity (1.5%).

### 4.2. Rapid Crop Establishment and Early Growth Under MLGS Optimization

Under MLGS-optimized conditions, all three candidate crops established successfully, demonstrating that the system provided a conducive environment during the critical post-transplant stage. Table 11 shows consistently high establishment performance across species, with acclimatization completed within 15 days. *A. cordifolia* established most rapidly, with 100% cutting survival and rooting achieved within 7 days, followed by earlier continuous harvest than in the control. *M. crystallinum* also performed well, showing earlier development of epidermal bladder cells, which suggests accelerated early morphological differentiation. Although *A. roxburghii* exhibited slightly slower acclimatization, it still maintained a high establishment rate and stable early vegetative growth.

### 4.3. Species-Specific Performance Under Optimized MLGS Conditions

#### 4.3.1. Enhanced Growth, Photosynthetic Performance, & Nutritional Quality in *Mesembryanthemum crystallinum*

*M. crystallinum* grown under optimized MLGS conditions showed marked improvements in growth, photosynthetic capacity, nutritional quality, and water-use efficiency compared with the control. Table 12 demonstrates that the optimized regime significantly enhanced biomass accumulation, net photosynthetic rate, nutrient content, and water-use efficiency, with the largest relative increases observed for potassium content, water-use efficiency, net photosynthetic rate, and dry weight. These responses were supported by large effect sizes and strong statistical significance. By contrast, MDA did not differ significantly between treatments, suggesting that the performance gains were achieved without detectable increases in oxidative stress. Consistent with these results, Figure 3 shows higher mean values for most measured traits under optimized MLGS conditions than under the control.

**Table 10.** Environmental control performance of the MLGS over 180 days of continuous operation, including target ranges, control stability, spatial uniformity, within-specification percentage, and disturbance recovery time for all monitored parameters.

Parameter	Target Range	Control Stability	CV (%)	Within-Spec (%)	Disturbance Recovery
Temperature	5–40°C	$\pm 0.8^\circ\text{C}$	2.3	98.7	$12.1 \pm 2.3$ min
Relative humidity	35–90%	$\pm 1.5\%$	3.1	97.9	$6.8 \pm 1.1$ min
$\text{CO}_2$ concentration	25–5000 ppm	25–35 ppm*	1.8	99.2	$8.3 \pm 1.4$ min
Airflow velocity	$0.1\text{--}1.0 \text{ m}\cdot\text{s}^{-1}$	$\pm 0.08 \text{ m}\cdot\text{s}^{-1}$	4.2	99.5	$3.2 \pm 0.8$ min
Light intensity (PPFD)	$0\text{--}3000 \mu\text{mol}\cdot\text{m}^{-2}\cdot\text{s}^{-1}$	$\pm 3\%$ calibrated	1.5	100	—
Root-zone temperature	5–40°C	$\pm 0.9^\circ\text{C}$	2.7	97.6	—
pH	4.8–8.0	$\pm 0.15$	2.1	98.2	—
EC	$0.5\text{--}5.0 \text{ dS}\cdot\text{m}^{-1}$	$\pm 0.4 \text{ dS}\cdot\text{m}^{-1}$	3.8	97.8	—

Note.\* $\text{CO}_2$  control stability expressed as standard deviation from setpoint during steady-state operation (Vaisala GMP252 sensor accuracy  $\pm 40$  ppm)

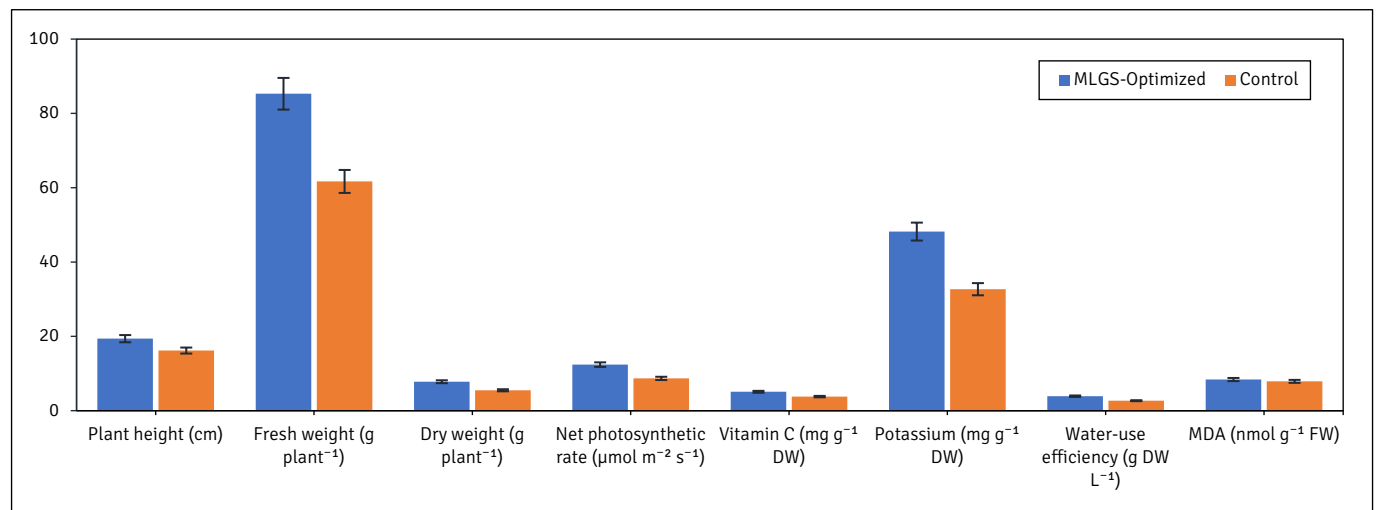
**Table 11.** Crop establishment success rates, acclimatization periods, and early growth observations for the three candidate species under MLGS-optimized conditions

Species	Establishment Success	Acclimatization Period	Early Growth Observations
<i>M. crystallinum</i>	95.0% (57/60 plants)	<15 days	Epidermal bladder cells appeared earlier in MLGS-optimized treatment (15 vs. 25 days in control)
<i>A. cordifolia</i>	100% (60/60 cuttings)	<7 days	Adventitious roots formed within 7 days; continuous harvest began at day 45 (MLGS-optimized) vs. day 60 (control)
<i>A. roxburghii</i>	97.10%	15 days	Leaf elongation 2–3 mm day <sup>-1</sup> initial phase; accelerated after day 60

**Table 12.** Performance parameters for *M. crystallinum* under optimized MLGS vs. control conditions (Mean ± SD, n = 3 biological replicates)

Parameter	MLGS-Optimized	Control	Change (%)	Cohen's d	p-value
Plant height (cm)	19.4 ± 1.8	16.2 ± 2.1	+19.8	1.64	<0.01
Fresh weight (g plant <sup>-1</sup> )	85.3 ± 6.4	61.7 ± 5.8	+38.2	3.84	<0.001
Dry weight (g plant <sup>-1</sup> )	7.8 ± 0.6	5.5 ± 0.5	+41.5	4.18	<0.001
Net photosynthetic rate (μmol m <sup>-2</sup> s <sup>-1</sup> )	12.4 ± 1.1	8.7 ± 0.9	+42.5	3.68	<0.001
Vitamin C (mg g <sup>-1</sup> DW)	5.1 ± 0.4	3.8 ± 0.3	+34.2	3.64	<0.01
Potassium (mg g <sup>-1</sup> DW)	48.2 ± 3.1	32.7 ± 2.8	+47.4	5.21	<0.001
Water-use efficiency (g DW L <sup>-1</sup> )	3.9 ± 0.3	2.7 ± 0.2	+44.2	4.66	<0.001
MDA (nmol g <sup>-1</sup> FW)	8.4 ± 1.2	7.9 ± 1.1	+6.3	0.43	0.18 (NS)

Note. DW = dry weight; FW = fresh weight; NS = not significant; Complete physiological and nutritional data for *M. crystallinum* (Suppl. Table S4).

**Figure 3.** Comparative performance of *Mesembryanthemum crystallinum* grown under optimized MLGS and control conditions.**Table 13.** Performance parameters for *A. cordifolia* under optimized MLGS vs. control conditions (Mean ± SD, n = 3 biological replicates)

Parameter	MLGS-Optimized	Control	Change (%)	Cohen's d	p-value
Vine elongation rate (cm day <sup>-1</sup> )	8.2 ± 1.1	5.9 ± 0.8	+38.9	2.38	<0.01
Fresh weight at 180 d (g plant <sup>-1</sup> )	285.6 ± 22.4	198.3 ± 18.7	+44.0	4.19	<0.01
Cumulative edible yield (g DW m <sup>-2</sup> )	312.4 ± 18.6	197.8 ± 15.3	+57.9	6.73	<0.001
Net photosynthetic rate (μmol m <sup>-2</sup> s <sup>-1</sup> )	18.7 ± 1.4	11.4 ± 1.1	+64.0	5.74	<0.001
Protein (% DW)	22.8 ± 1.4	18.3 ± 1.2	+24.6	3.47	<0.001
Omega-3 fatty acids (% DW)	1.2 ± 0.2	0.9 ± 0.1	+33.3	1.84	<0.01
Vitamin C (mg g <sup>-1</sup> DW)	3.9 ± 0.4	2.9 ± 0.3	+34.5	2.77	<0.01
Water-use efficiency (g DW L <sup>-1</sup> )	4.8 ± 0.4	3.1 ± 0.3	+54.8	4.82	<0.001

Parameter	MLGS-Optimized	Control	Change (%)	Cohen's d	p-value
MDA (nmol g <sup>-1</sup> FW)	9.2 ± 1.4	8.6 ± 1.3	+7.0	0.44	0.22 (NS)

Note. DW = dry weight; FW = fresh weight; NS = not significant; Complete physiological and nutritional data for *A. cordifolia* (Suppl. Table S5).

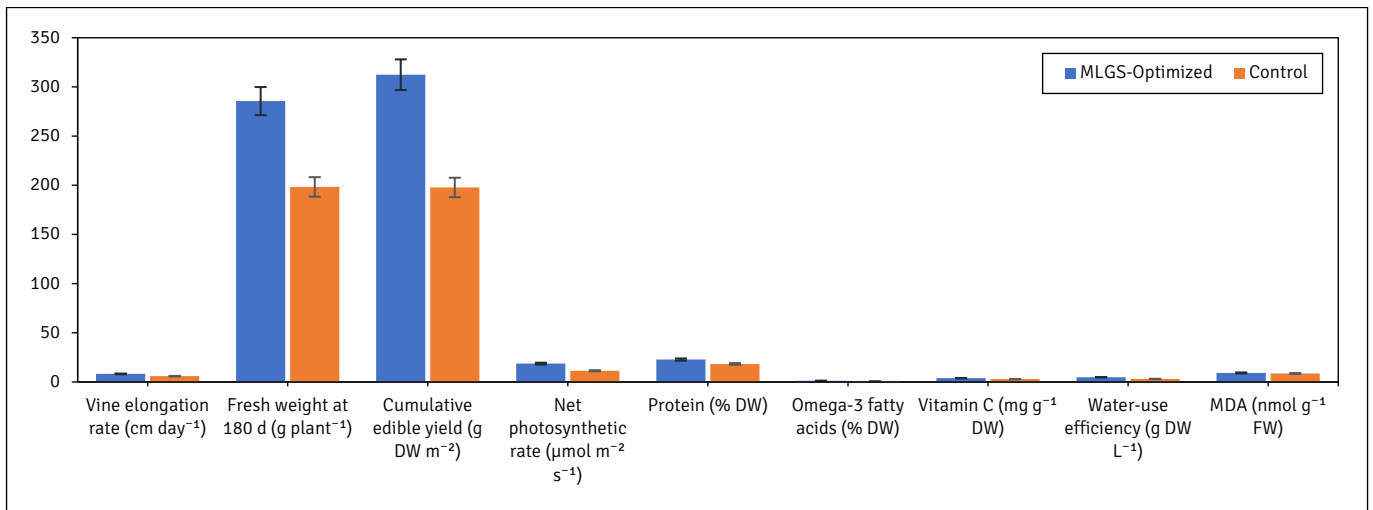


**Figure 4.** Comparative performance of *Anredera cordifolia* under optimized MLGS and control conditions.

**Table 14.** Performance parameters for *A. roxburghii* under optimized MLGS vs. control conditions (Mean ± SD, n = 3 biological replicates)

Parameter	MLGS-Optimized	Control	Change (%)	Cohen's d	p-value
Establishment success (%)	97.1 ± 2.3	82.3 ± 4.1	+18.0	4.41	<0.01
Plant height at 90 d (cm)	13.8 ± 1.1	10.2 ± 1.4	+35.3	2.83	<0.001
Fresh weight (g plant <sup>-1</sup> )	9.4 ± 0.8	5.8 ± 0.7	+62.1	4.78	<0.001
Root surface area (cm <sup>2</sup> )	42.6 ± 4.8	28.1 ± 3.7	+51.6	3.38	<0.001
Polysaccharides (% DW)	26.8 ± 1.7	19.4 ± 1.5	+38.1	4.60	<0.001
Flavonoids (mg g <sup>-1</sup> DW)	6.4 ± 0.5	4.4 ± 0.4	+45.5	4.38	<0.001
Alkaloids (mg g <sup>-1</sup> DW)	1.82 ± 0.14	1.31 ± 0.11	+38.9	4.02	<0.001
Antioxidant IC <sub>50</sub> (mg mL <sup>-1</sup> )	0.41 ± 0.04	0.67 ± 0.06	-38.8*	5.05	<0.001
Water-use efficiency (g DW L <sup>-1</sup> )	3.9 ± 0.3	3.1 ± 0.2	+25.3	3.10	<0.01
MDA (nmol g <sup>-1</sup> FW)	7.1 ± 1.0	6.8 ± 0.9	+4.4	0.31	0.31 (NS)

Note. Lower IC<sub>50</sub> indicates stronger antioxidant capacity; DW = dry weight; FW = fresh weight; NS = not significant; Complete physiological and biochemical data for *A. roxburghii* (Suppl. Table S6).

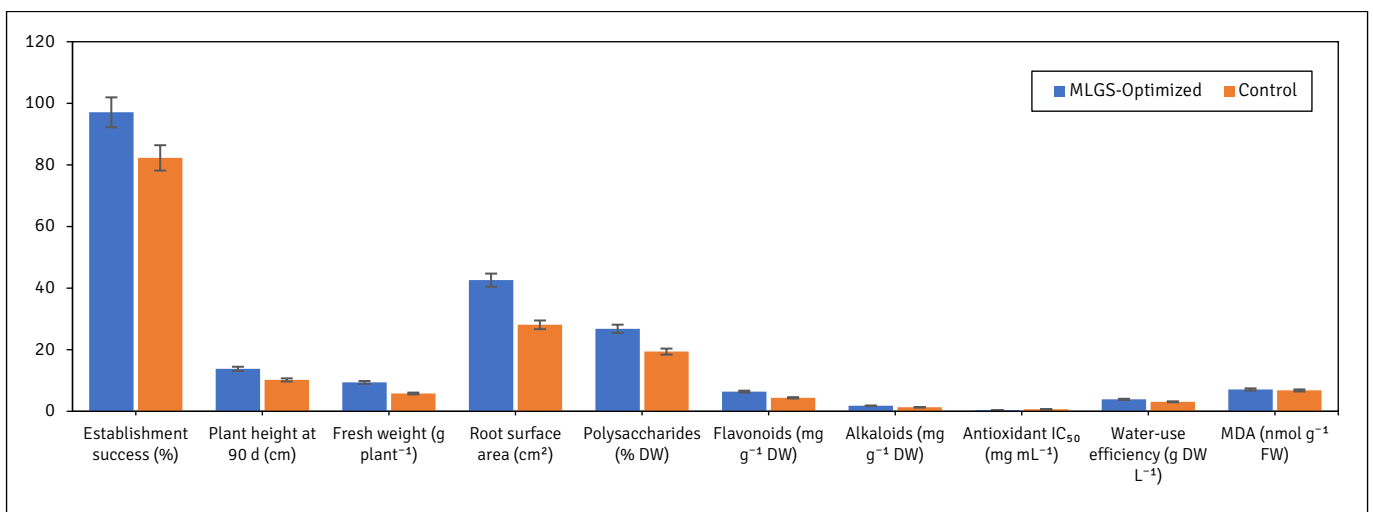


**Figure 5.** Comparative performance of *Anoectochilus roxburghii* under optimized MLGS and control conditions.

#### 4.3.2. Strong Productivity and Nutritional Gains in *Anredera cordifolia*

*A. cordifolia* exhibited the strongest overall response to optimized MLGS conditions among the three species, with substantial improvements in vegetative growth, edible yield, photosynthetic capacity, and nutritional quality. Table 13 shows that the optimized treatment resulted in broad and statistically significant gains across almost all measured traits. The most pronounced increases were observed in net photosynthetic rate, cumulative edible yield, and water-use efficiency, highlighting a strong enhancement in overall productivity. Nutritional quality was also improved, with higher protein, omega-3 fatty acid, and vitamin C contents than in the control. By contrast, MDA remained unchanged between treatments, suggesting that the increased productivity was not accompanied by detectable additional oxidative stress. Figure 4 further confirms this pattern, with higher mean values under optimized MLGS conditions for most measured variables.

#### 4.3.3. Growth and Bioactive Enhancement in *A. roxburghii* Under Optimized MLGS Conditions

*A. roxburghii* grown under optimized MLGS conditions showed superior establishment, vegetative growth, root development, and bioactive compound accumulation compared with the control. Table 14 indicates significant improvements in fresh weight, plant height, root surface area, and the accumulation of polysaccharides, flavonoids,

and alkaloids under the optimized regime. Antioxidant capacity was also enhanced, as reflected by a lower IC<sub>50</sub> value, while MDA remained unchanged, indicating no detectable increase in oxidative stress.

Nevertheless, these results require cautious interpretation because *A. roxburghii* is an understory species with a reported optimal light range of 50–150  $\mu\text{mol m}^{-2} \text{s}^{-1}$ , whereas the control treatment applied 200  $\mu\text{mol m}^{-2} \text{s}^{-1}$ . Accordingly, part of the treatment difference may be attributable to suboptimal control conditions, meaning that the response likely represents the combined effects of MLGS optimization and a less favorable baseline environment. Figure 5 supports this overall trend.

#### 4.4. Nutritional Profiles of MLGS-Grown Species

Under optimized MLGS conditions, the three species displayed distinct but complementary nutritional profiles, indicating their potential for different functional roles in diversified crop systems. Table 15 shows clear nutritional specialization among the species. *A. cordifolia* had the highest protein, lipid, and omega-3 fatty acid contents, indicating strong value as a macronutrient-rich crop. *M. crystallinum* was distinguished by its high calcium and vitamin C contents, supporting its contribution as a mineral- and micronutrient-dense species. In contrast, *A. roxburghii* was characterized primarily by its substantial polysaccharide, flavonoid, and alkaloid contents, emphasizing its role as a bioactive-rich medicinal crop.

**Table 15.** Nutritional composition of MLGS-grown crops (dry weight basis).

Component	<i>M. crystallinum</i>	<i>A. cordifolia</i>	<i>A. roxburghii</i>
Protein (% DW)	12.4 ± 0.8	22.8 ± 1.4	8.3 ± 0.6
Lipid (% DW)	2.1 ± 0.3	3.8 ± 0.4	1.9 ± 0.2
Calcium (mg g <sup>-1</sup> DW)	22.4 ± 1.9†	4.2 ± 0.3	2.8 ± 0.2
Vitamin C (mg g <sup>-1</sup> DW)	5.1 ± 0.4	3.9 ± 0.4	2.4 ± 0.2
Omega-3 fatty acids (% DW)	0.8 ± 0.1	1.2 ± 0.2	0.4 ± 0.1
Polysaccharides (% DW)	—	—	26.8 ± 1.7
Flavonoids (mg g <sup>-1</sup> DW)	—	—	6.4 ± 0.5
Alkaloids (mg g <sup>-1</sup> DW)	—	—	1.82 ± 0.14

Note. This value, reported in Suppl. Table S4, supersedes the previously reported 8.7 mg g<sup>-1</sup>. All calcium values have been verified and harmonized throughout the manuscript.

**Table 16.** Water-use efficiency (g dry weight per liter water consumed) of three MLGS-grown species under optimized and control conditions, with percentage improvement

Species	MLGS-Optimized (g DW L <sup>-1</sup> )	Control (g DW L <sup>-1</sup> )	Improvement (%)
<i>Mesembryanthemum crystallinum</i>	3.9 ± 0.3	2.7 ± 0.2	+44.2
<i>Anredera cordifolia</i>	4.8 ± 0.4	3.1 ± 0.3	+54.8
<i>Anoectochilus roxburghii</i>	3.9 ± 0.3	3.1 ± 0.2	+25.3

Note. Values previously reported in Suppl. tables as 24.6 g kg<sup>-1</sup> water for *A. cordifolia* and 31.2 g kg<sup>-1</sup> water for *A. roxburghii* have been converted to g L<sup>-1</sup> (1 kg water = 1 L water) and harmonized with the main tables. All values are now presented in consistent units throughout the manuscript.

**Table 17.** Waste processing performance of three candidate crops: nitrogen removal, phosphorus removal, crop residue biodegradability, and final urea concentration after 30-day simulated astronaut waste liquid treatment.

Parameter	<i>M. crystallinum</i>	<i>A. cordifolia</i>	<i>A. roxburghii</i>
Nitrogen removal (% , 30 d)	71.4 ± 4.8	78.9 ± 5.2	58.3 ± 4.1
Phosphorus removal (% , 30 d)	62.1 ± 4.3	69.8 ± 5.1	47.2 ± 3.9
Residue biodegradability (% mass loss, 30 d)	65 ± 5	58 ± 4	52 ± 5
Final urea concentration (g L <sup>-1</sup> , 30 d)	<0.18	<0.18	<0.18

**Table 18.** Microbial community diversity and food safety indicators for MLGS-optimized vs. control cultivation conditions: rhizosphere and phyllosphere Shannon diversity indices, total culturable microbial counts, and pathogen detection results

Parameter	MLGS-Optimized	Control
Rhizosphere bacterial diversity (Shannon index)	4.82 ± 0.31	3.64 ± 0.28
Phyllosphere bacterial diversity (Shannon index)	2.94 ± 0.22	3.18 ± 0.25
Total culturable microbes (CFU g <sup>-1</sup> )	3.2 × 10 <sup>3</sup> ± 0.4 × 10 <sup>3</sup>	8.7 × 10 <sup>3</sup> ± 1.1 × 10 <sup>3</sup>
Pathogen detection (Salmonella, E. coli, Listeria)	Not detected in any sample	Not detected in any sample

Note. Complete microbiome analysis (beta diversity, PERMANOVA results) is provided in Suppl. Table S9, S10 and S11.

#### 4.5. Resource Efficiency and Closed-Loop Integration Potential

##### 4.5.1. Water-Use efficiency gains under MLGS

To ensure consistency, all water-use efficiency (WUE) values are expressed as grams of dry weight per liter of water consumed (g DW L<sup>-1</sup>). Table 16 compares WUE under MLGS-optimized and control conditions and quantifies the relative improvement for each species. MLGS optimization improved WUE in all three species. *A. cordifolia* showed both the highest absolute WUE and the greatest percentage increase, indicating the strongest response to optimized cultivation. *M. crystallinum* also showed a marked gain, whereas *A. roxburghii* exhibited a smaller but still meaningful improvement.

##### 4.5.2. Waste processing and nutrient recovery capacity

Integration into controlled ecological life-support systems also requires compatibility with waste-processing and nutrient-recycling subsystems. To assess this capacity, nitrogen removal, phosphorus removal, residue biodegradability, and residual urea concentration were measured after 30 days of simulated astronaut waste liquid treatment. Table 17 indicates that all three species contributed to nutrient recovery and waste stabilization, although their relative performance differed. *A. cordifolia* showed the highest nitrogen and phosphorus removal efficiencies, whereas *M. crystallinum* had the greatest residue biodegradability. *A. roxburghii* showed lower removal efficiencies but still achieved substantial nutrient reduction. Final urea concentrations fell below 0.18 g L<sup>-1</sup> in all treatments, supporting the feasibility of integrating these crops into CELSS waste-processing and resource-recycling subsystems.

#### 4.6. Microbial Stability and Food Safety Under MLGS Optimization

Microbiological stability and food safety are critical considerations for controlled-environment crop production. To evaluate these aspects, microbial diversity, total culturable microbial counts, and pathogen presence were compared between MLGS-optimized and control conditions. As shown in Table 18, MLGS-optimized cultivation was associated with higher rhizosphere bacterial diversity and lower total culturable microbial counts than the control. Phyllosphere diversity was slightly lower under optimized conditions, but no foodborne pathogens were detected in any sample under either treatment.

#### 4.7. Cross-Species Comparative Summary

Under optimized MLGS conditions, *A. cordifolia* exhibited the greatest biomass-related improvements, with fresh weight and cumulative yield increasing by 44% and 58%, respectively, and it showed the highest water-use efficiency (4.8 g DW L<sup>-1</sup>). In contrast, *A. roxburghii* demonstrated the largest increases in the measured bioactive compounds, including polysaccharides (+38%), flavonoids (+45%), and alkaloids (+39%). *M. crystallinum* had the highest calcium concentration (22.4 mg g<sup>-1</sup> DW) and showed a substantial capacity for salt accumulation, retaining 34.7% of the supplied salt. Malondialdehyde (MDA) levels did not differ significantly between treatments in any species, indicating that the optimized MLGS conditions did not induce additional oxidative stress.

Figure 6 Normalized comparative performance of the three species in terms of biomass production, photosynthetic rate, nutritional quality, water-use efficiency, and bioactive compound accumulation. Values are expressed as percentages of the maximum observed

for each metric ( $n = 3$  biological replicates). *A. cordifolia* showed the strongest performance in biomass production and water-use efficiency, whereas *A. roxburghii* exhibited the highest bioactive compound levels. *M. crystallinum* displayed an intermediate overall profile, with notably high mineral content.

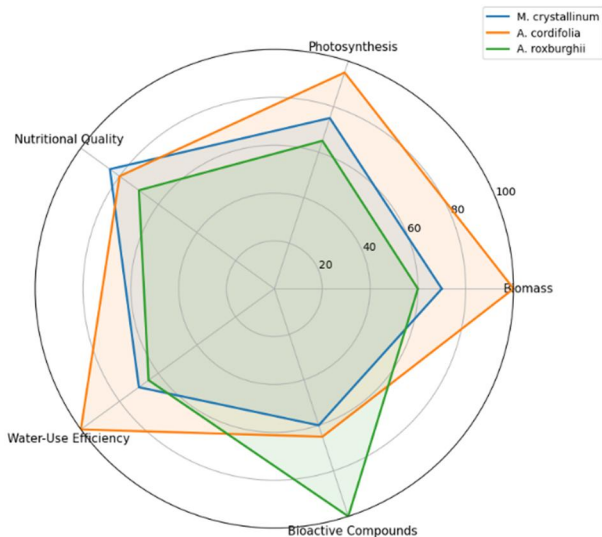


**Figure 6.** Comparing Normalized cross-species performance summary.

## 5. DISCUSSION

### 5.1. Platform Performance and Environmental Control Capabilities

The 180-day continuous operation demonstrates that the Micro-Lunar Greenhouse System (MLGS) can maintain a stable cultivation environment over durations that are relevant for pre-integrated CELSS research. Environmental deviations remained narrow, and the system recovered rapidly from CO<sub>2</sub> disturbances, indicating that MLGS is not merely a short-term plant growth chamber but a controllable experimental platform capable of supporting reproducible crop evaluation. In the context of CELSS and bioregenerative life support systems, such environmental stability is crucial because long-duration missions require crop systems that are productive, operationally reliable, and sufficiently modular for repeated ground validation before integration with other life-support subsystems [43], [92], [93]. The low spatial variation observed across cultivation zones is also important because it reduces the possibility that interspecific comparisons are confounded by local microclimatic heterogeneity. Taken together, these findings suggest that MLGS can function as an intermediate platform between conventional laboratory growth chambers and larger integrated CELSS research infrastructures. However, the present experimental design also indicates that the crop responses discussed below should be interpreted as the combined outcome of

platform stability and species-specific environmental optimization, rather than as a hardware effect alone.

### 5.2. Species-Specific Responses

The three tested species responded differently to optimized MLGS conditions, which is consistent with the established principle that plant performance in controlled environments is strongly species-dependent. In *Mesembryanthemum crystallinum*, the increases in biomass, photosynthetic rate, and water-use efficiency are physiologically plausible under elevated CO<sub>2</sub> and tightly regulated hydroponic cultivation. Elevated CO<sub>2</sub> generally enhances carbon assimilation in C3 plants, but the magnitude of the response depends on interactions with temperature, nutrient supply, source-sink balance, and light environment [94]. Therefore, the stronger response observed here likely reflects the combined optimization of several environmental factors rather than a single CO<sub>2</sub> effect. The observed increases in potassium and vitamin C are also broadly consistent with previous evidence that halophytic crops grown in soilless systems can maintain strong nutritional quality under controlled cultivation [95].

Among the three species, *Anredera cordifolia* showed the greatest productivity gains, including fresh biomass, cumulative edible yield, and photosynthetic performance. Because the reported increases in protein, omega-3 fatty acids, and vitamin C exceed what is commonly attributed to CO<sub>2</sub> enrichment alone, a more cautious interpretation is that the species benefited from synergistic optimization of atmospheric, thermal, and nutritional conditions. This interpretation aligns with controlled-environment literature showing that crop responses under elevated CO<sub>2</sub> are strongly modulated by accompanying environmental controls rather than by CO<sub>2</sub> concentration in isolation [92], [94]. Thus, *A. cordifolia* appears to be a promising candidate for CELSS-oriented cultivation not only because of its productivity, but also because of its favorable nutritional profile under optimized management.

The response of *Anoectochilus roxburghii* requires more careful interpretation. This species is a shade-adapted medicinal understory plant, and part of its apparent advantage under MLGS may reflect the fact that the control treatment used a light intensity that was not optimal for its ecophysiology. Even so, the increases in polysaccharides, flavonoids, and alkaloids are consistent with previous studies showing that the light environment strongly regulates morphology and bioactive compound accumulation in *A. roxburghii* [96]. More broadly, controlled-environment systems are increasingly recognized as suitable platforms for medicinal plants because precise regulation of light, temperature, humidity, CO<sub>2</sub>, and nutrients can improve the consistency and concentration of specialized metabolites [97]. Accordingly, the MLGS results for *A. roxburghii* are best interpreted as evidence of the platform's value for

medicinal crop optimization, while still acknowledging that the control regime may have exaggerated treatment differences.

### 5.3. Nutritional Quality and Resource-Use Efficiency

Beyond biomass enhancement, the MLGS findings are important because they address several metrics central to CELSS feasibility, namely water-use efficiency, nutrient recovery, carbon fixation, and nutritional complementarity across species. In hydroponic systems, precise nutrient-solution management is a major determinant of both water-use efficiency and nutrient-use efficiency, especially in recirculating cultivation systems [69]. From this perspective, the reported values of water-use efficiency and N/P recovery are not only agronomically favorable but also relevant to closed-loop habitat design, where efficient recycling of water and nutrients directly affects system mass, logistics, and operational sustainability [93]. Likewise, the measured CO<sub>2</sub> fixation efficiencies fall within physiologically credible expectations for C3 plants cultivated under elevated CO<sub>2</sub>, suggesting that the optimized MLGS package supported effective photosynthesis without obvious evidence of metabolic dysfunction [94].

The three species also contributed complementary nutritional functions: *A. cordifolia* supplied relatively high protein, *M. crystallinum* contributed mineral richness, and *A. roxburghii* provided medicinally relevant phytochemicals. This complementarity is important because CELSS crop portfolios should not be selected on the basis of yield alone; they must also contribute to dietary diversity, nutritional adequacy, and health-supporting functions over long mission durations [92]. Thus, the present findings support the concept of multi-species crop assemblages as a more realistic direction for future CELSS food-system design.

### 5.4. Microbial Safety and System Integration

The lower total culturable microbial loads in MLGS-grown samples are encouraging from a food-safety standpoint, especially because crops in closed habitats may often be consumed fresh or minimally processed. At the same time, the higher diversity of rhizosphere bacteria suggests that tighter environmental control did not simply suppress microbial life, but may instead have supported a more structured and potentially beneficial root-associated microbial community. This interpretation is consistent with rhizosphere microbiome research showing that microbial diversity can contribute to plant health, nutrient acquisition, and resilience, provided that pathogenic taxa are excluded [98]. However, the results should still be interpreted cautiously. Even in controlled hydroponic systems, microbial food-safety risks are not eliminated; they may instead shift toward water, nutrient solution, equipment, and worker-associated contamination pathways [99]. Therefore, the microbial results reported here should be framed as promising but preliminary, and

they justify longer-term monitoring of community succession, pathogen exclusion, and sanitation performance under more operationally realistic CELSS conditions.

### 5.5. Comparison with Existing Platforms

From a methodological perspective, MLGS appears to occupy an important intermediate niche in CELSS research infrastructure. Previous space-crop literature has emphasized the need for experimental platforms that are more physiologically meaningful than standard growth chambers, yet more flexible and less resource-intensive than large integrated life-support demonstrators [92], [93]. In this regard, MLGS offers several valuable features: coupled control of temperature, humidity, CO<sub>2</sub>, light environment, and airflow; demonstrated long-term operational stability; and sufficient modularity to support comparative crop assessment under reproducible conditions. Its main contribution, therefore, is not to replace fully integrated CELSS facilities, but to provide a reliable mid-scale platform for screening crop candidates and environmental recipes before larger-scale system integration. This makes MLGS particularly valuable for iterative optimization studies, where experimental throughput, reproducibility, and cost remain critical considerations.

## 6. LIMITATIONS AND FUTURE WORK

Several limitations should be explicitly acknowledged. First, the comparison between optimized MLGS conditions and standard laboratory conditions does not isolate platform effects from environmental optimization effects; consequently, the present study demonstrates the performance of an optimized cultivation package rather than the independent effect of the platform itself. Second, the control light regime used for *A. roxburghii* may have amplified treatment differences because the species is highly sensitive to the quality and intensity of incident light [96]. Third, although 180 days of operation is substantial from an engineering perspective, it remains short relative to the timeframes relevant to lunar or Martian habitation scenarios. Fourth, only three species were tested, all in monoculture and under Earth gravity, which limits direct extrapolation to mixed-species and partial-gravity BLSS operation. Finally, MLGS was evaluated as a stand-alone cultivation platform rather than as part of a materially integrated CELSS architecture. Future studies should therefore prioritize factorial designs that separate hardware and environmental effects, longer-duration trials, inclusion of staple and additional functional crops, multi-species cultivation, partial-gravity analog testing, and direct coupling to waste-processing and nutrient-recycling modules [92], [93]. In addition, claims of scalability should ultimately be

supported by energy-use accounting, mass-balance analysis, and life-cycle assessment.

## 7. CONCLUSION

This study demonstrates that the Micro-Lunar Greenhouse System (MLGS) is a stable, modular, and reproducible mid-scale platform for CELSS-oriented crop screening, capable of maintaining tightly controlled environmental conditions over 180 days while supporting comparative evaluation of functionally diverse species. Under species-optimized MLGS conditions, *Mesembryanthemum crystallinum*, *Anredera cordifolia*, and *Anoectochilus roxburghii* exhibited consistent improvements in biomass production, photosynthetic performance, nutritional or bioactive quality, and water-use efficiency relative to standard laboratory cultivation, while also showing meaningful potential for nutrient recovery from simulated waste streams and acceptable microbiological safety. Taken together, these findings position the MLGS as an effective methodological bridge between large integrated CELSS facilities and conventional growth chambers, enabling standardized long-duration screening of candidate crops for space agriculture. However, because the present comparison combined platform operation with species-specific environmental optimization, the results should be interpreted as evidence for the performance of an integrated cultivation package rather than the isolated effect of the platform alone; accordingly, future studies should separate hardware and environmental effects through factorial designs, extend operational timescales, and test broader crop portfolios under more fully integrated closed-loop conditions.

### ACKNOWLEDGMENTS

The authors would like to express their deepest gratitude to the University, our colleagues and laboratory support for their supported greenhouse operation, sensor calibration, and sample processing.

### CONFLICTS OF INTEREST

The authors declare that no conflicts of interest are associated with this study. All aspects of the research were conducted with the utmost integrity and transparency.

### DATA AVAILABILITY

The datasets utilized and analyzed during this research are available from the corresponding author upon reasonable request.

### ETHICAL STATEMENTS

Not applicable. This study involved plant cultivation, environmental control experiments, and microbial analyses only; it did not involve human participants or vertebrate animals. All procedures were conducted in accordance with institutional laboratory safety and biosafety regulations.

### FUNDING

This research was conducted without financial support. The authors confirm that no funding was received for this study's research, analysis, or publication.

## REFERENCES

- [1] V. Maiwald, K. Kyunghwan, V. Vrakking, and C. Zeidler, "From Antarctic prototype to ground test demonstrator for a lunar greenhouse," *Acta Astronaut.*, vol. 212, pp. 246–260, 2023, <https://doi.org/10.1016/j.actaastro.2023.08.012>
- [2] J. W. Prats, D. K. S. Souffront, M. S. B. Bhaskar, and K. Jayachandran, "Development of a Controlled-environment Plant Growth Chamber Using a Shipping Container for Industrial Hemp (*Cannabis sativa* L.) Cultivation," *Horttechnology*, vol. 36, no. 1, pp. 24–30, 2026, <https://doi.org/10.21273/HORTECH05767-25>
- [3] J. Guerrero-Sánchez et al., "Design and Implementation of a Low-Cost Controlled-Environment Growth Chamber for Vegetative Propagation of Mother Plants," *AgriEngineering*, vol. 7, no. 6, p. 177, 2025, <https://doi.org/10.3390/agriengineering7060177>
- [4] F. Ben Othman, S. Delattainant, A. L. Alexandre, M. Roque, and C. Roque, "Development and evaluation of a climatic chamber with the potential to enhance plant resilience and optimize agricultural productivity," *Therm. Sci. Eng. Prog.*, vol. 62, p. 103645, 2025, <https://doi.org/10.1016/j.tsep.2025.103645>
- [5] G. Metelli et al., "Design of a modular controlled unit for the study of bioprocesses: Towards solutions for Bioregenerative Life Support Systems in space," *Life Sci. Sp. Res.*, vol. 36, pp. 8–17, 2023, <https://doi.org/10.1016/j.lssr.2022.10.006>
- [6] V. De Micco et al., "Plant and microbial science and technology as cornerstones to Bioregenerative Life Support Systems in space," *npj Microgravity*, vol. 9, no. 1, p. 69, 2023, <https://doi.org/10.1038/s41526-023-00317-9>
- [7] D. Marshall Porterfield et al., "Critical investments in bioregenerative life support systems for bioastronautics and sustainable lunar exploration," *npj Microgravity*, vol. 11, no. 1, p. 57, 2025, <https://doi.org/10.1038/s41526-025-00518-4>
- [8] H. C. Wright et al., "Space controlled environment agriculture offers pathways to improve the sustainability of controlled environmental agriculture on Earth," *Nat. Food*, vol. 4, no. 8, pp. 648–653, 2023, <https://doi.org/10.1038/s43016-023-00819-5>
- [9] R. Fritsche et al., "Space Crop Considerations for Human Exploration," *National Aeronautics and Space Administration*, 2024. [Online]. Available: <https://ntrs.nasa.gov/citations/20250001897>
- [10] L. Poulet et al., "Large-Scale Crop Production for the Moon and Mars: Current Gaps and Future Perspectives," *Front. Astron. Sp. Sci.*, vol. 8, p. 733944, 2022, <https://doi.org/10.3389/fspas.2021.733944>
- [11] S. Chen, A. Liu, F. Tang, P. Hou, Y. Lu, and P. Yuan, "A Review of Environmental Control Strategies and Models for Modern Agricultural Greenhouses," *Sensors*, vol. 25, no. 5, p. 1388, 2025, <https://doi.org/10.3390/s25051388>
- [12] E. Iddio, L. Wang, Y. Thomas, G. McMorro, and A. Denzer, "Energy efficient operation and modeling for greenhouses: A literature review," *Renew. Sustain. Energy Rev.*, vol. 117, p. 109480, 2020, <https://doi.org/10.1016/j.rser.2019.109480>
- [13] P. Suwanichakasem, A. Idnurm, J. Selby-Pham, R. Walker, and B. A. Boughton, "Root-TRAPP: a modular plant growth

- device to visualize root development and monitor growth parameters, as applied to an elicitor response of *Cannabis sativa*,” *Plant Methods*, vol. 18, no. 1, p. 46, 2022, <https://doi.org/10.1186/s13007-022-00875-1>
- [14] N. H. Doddrell, T. Lawson, C. A. Raines, C. Wagstaff, and A. J. Simkin, “Feeding the world: impacts of elevated [CO<sub>2</sub>] on nutrient content of greenhouse grown fruit crops and options for future yield gains,” *Hortic. Res.*, vol. 10, no. 4, p. uhad026, 2023, <https://doi.org/10.1093/hr/uhad026>
- [15] H. Hamidane et al., “Constrained temperature and relative humidity predictive control: Agricultural greenhouse case of study,” *Inf. Process. Agric.*, vol. 11, no. 3, pp. 409–420, 2024, <https://doi.org/10.1016/j.inpa.2023.04.003>
- [16] L. Yao et al., “High air humidity dampens salicylic acid pathway and NPR1 function to promote plant disease,” *EMBO J.*, vol. 42, no. 21, p. EMBJ2023113499, 2023, <https://doi.org/10.15252/embj.2023113499>
- [17] J. Zhang et al., “Harnessing the plant microbiome to promote the growth of agricultural crops,” *Microbiol. Res.*, vol. 245, p. 126690, 2021, <https://doi.org/10.1016/j.micres.2020.126690>
- [18] S. Compant et al., “Harnessing the plant microbiome for sustainable crop production,” *Nat. Rev. Microbiol.*, vol. 23, no. 1, pp. 9–23, 2025, <https://doi.org/10.1038/s41579-024-01079-1>
- [19] E. Peiro et al., “Air Distribution in a Fully-Closed Higher Plant Growth Chamber Impacts Crop Performance of Hydroponically-Grown Lettuce,” *Front. Plant Sci.*, vol. 11, p. 537, 2020, <https://doi.org/10.3389/fpls.2020.00537>
- [20] F. B. Salisbury, J. I. Gitelson, and G. M. Lisovsky, “Bios-3: Siberian experiments in bioregenerative life support,” *Bioscience*, vol. 47, no. 9, pp. 575–585, 1997, <https://doi.org/10.2307/1313164>
- [21] Y. Tako et al., “CEEF: Closed Ecology Experiment Facilities,” *Gravitational Sp. Biol.*, vol. 23, no. 2, pp. 13–24, 2010.
- [22] S. Mallick, F. Airdali, A. Dabiri, C. Sun, and B. De Schutter, “Reinforcement learning-based model predictive control for greenhouse climate control,” *Smart Agric. Technol.*, vol. 10, p. 100751, 2025, <https://doi.org/10.1016/j.atech.2024.100751>
- [23] X. Han et al., “Design and Evaluation of an Innovative Thermoelectric-Based Dehumidifier for Greenhouses,” *Agronomy*, vol. 15, no. 5, p. 1194, 2025, <https://doi.org/10.3390/agronomy15051194>
- [24] Y. Fu et al., “A case for supporting human long-term survival on the moon: ‘Lunar Palace 365’ mission,” *Acta Astronaut.*, vol. 228, pp. 131–140, 2025, <https://doi.org/10.1016/j.actaastro.2024.12.002>
- [25] S. A. Wolff, L. H. Coelho, I. Karoliussen, and A. I. K. Jost, “Effects of the extraterrestrial environment on plants: Recommendations for future space experiments for the MELiSSA higher plant compartment,” *Life*, vol. 4, no. 2, pp. 189–204, 2014, <https://doi.org/10.3390/life4020189>
- [26] Y. Tako, S. Tsuga, T. Tani, R. Arai, O. Komatsubara, and M. Shinohara, “Carbon flow in an artificial ecosystem comprised of crew, goats and crops for three 1-week confined habitation experiments using CEEF,” *SAE Tech. Pap.*, pp. 174–180, 2006, <https://doi.org/10.4271/2006-01-2075>
- [27] T. Shimamiya et al., “Air circulation confinement experiments in the CEEF: Physiological status in econauts through repeated seven-day habitations,” *SAE Technical Paper*, 2006. <https://doi.org/10.4271/2006-01-2294>
- [28] T. Zhao, G. Liu, D. Liu, Y. Yi, B. Xie, and H. Liu, “Water recycle system in an artificial closed ecosystem – Lunar Palace 1: Treatment performance and microbial evolution,” *Sci. Total Environ.*, vol. 806, p. 151370, 2022, <https://doi.org/10.1016/j.scitotenv.2021.151370>
- [29] A. Guney and O. Cakir, “Design and Temperature Control of a Novel Aeroponic Plant Growth Chamber,” *Electron.*, vol. 14, no. 14, p. 2801, 2025, <https://doi.org/10.3390/electronics14142801>
- [30] W. Zhang, “Greenhouse monitoring system integrating NB-IOT technology and a cloud service framework,” *Nonlinear Eng.*, vol. 13, no. 1, p. 20240053, 2024, <https://doi.org/10.1515/nleng-2024-0053>
- [31] J. Hu, S. Li, H. Liu, and D. Hu, “Reliability and lifetime estimation of bioregenerative life support system based on 370-day closed human experiment of lunar palace 1 and Monte Carlo simulation,” *Acta Astronaut.*, vol. 202, pp. 609–616, 2023, <https://doi.org/10.1016/j.actaastro.2022.11.021>
- [32] H. Liu, Z. Yao, and H. Liu, “Human lunar base: ‘Lunar Palace 1’ team of Beihang University unveils China’s ‘Lunar Palace’ plan,” *Innov.*, vol. 5, no. 2, p. 100592, 2024, <https://doi.org/10.1016/j.xinn.2024.100592>
- [33] A. H. Morsy, G. D. Massa, R. C. Morrow, R. M. Wheeler, M. A. Elsysy, and C. A. Mitchell, “Leaf yield and mineral content of mizuna in response to cut-and-come-again harvest, substrate particle size, and fertilizer formulation in a simulated spaceflight environment,” *Life Sci. Sp. Res.*, vol. 40, pp. 106–114, 2024, <https://doi.org/10.1016/j.lssr.2023.09.005>
- [34] E. W. Darby, S. P. Armstrong, and K. J. Walters, “Bioregenerative dietary supplementation in space: Brassica rapa var. nipposinica and other Brassica cultivars,” *Life Sci. Sp. Res.*, vol. 42, pp. 140–147, 2024, <https://doi.org/10.1016/j.lssr.2023.12.002>
- [35] C. J. Spenn et al., “The microbial communities of a tomato crop grown in Veggie under different lighting regimes on the International Space Station,” *Life Sci. Sp. Res.*, 2026, <https://doi.org/10.1016/j.lssr.2026.01.010>
- [36] Y. Shen et al., “Research on a microgravity-adapted controlled-release fertilizer for space plant cultivation and its application experiments in the space station,” *Life Sci. Sp. Res.*, vol. 48, pp. 232–241, 2026, <https://doi.org/10.1016/j.lssr.2025.09.004>
- [37] J. M. Bunchek et al., “Pick-and-eat space crop production flight testing on the International Space Station,” *J. Plant Interact.*, vol. 19, no. 1, p. 2292220, 2024, <https://doi.org/10.1080/17429145.2023.2292220>
- [38] R. M. Wheeler et al., “Effects of elevated and super-elevated carbon dioxide on salad crops for space,” *J. Plant Interact.*, vol. 19, no. 1, p. 2292219, 2023, <https://doi.org/10.1080/17429145.2023.2292219>
- [39] A. J. Burgess, R. Pranggono, M. Escribà-Gelonch, and V. Hessel, “Biofortification for space farming: Maximising nutrients using lettuce as a model plant,” *Futur. Foods*, vol. 9, p. 100317, 2024, <https://doi.org/10.1016/j.fufo.2024.100317>
- [40] K. H. Hasenstein, S. G. A. Moinuddin, A. Berim, L. B. Davin, and N. G. Lewis, “Glucosinolate and Sugar Profiles in Space-Grown Radish,” *Plants*, vol. 14, no. 13, p. 2063, 2025, <https://doi.org/10.3390/plants14132063>
- [41] K. H. Hasenstein, S. P. John, and J. P. Vandenbrink, “Assessing Radish Health during Space Cultivation by

- Gene Transcription,” *Plants*, vol. 12, no. 19, p. 3458, 2023, <https://doi.org/10.3390/plants12193458>
- [42] M. E. Maffei et al., “The physiology of plants in the context of space exploration,” *Commun. Biol.*, vol. 7, no. 1, p. 1311, 2024, <https://doi.org/10.1038/s42003-024-06989-7>
- [43] L. L. Fountain et al., “Expanding frontiers: harnessing plant biology for space exploration and planetary sustainability,” *New Phytol.*, vol. 249, no. 2, pp. 656–669, 2026, <https://doi.org/10.1111/nph.70662>
- [44] J. M. Ortega-Hernandez et al., “Key factors in developing controlled closed ecosystems for lunar missions,” *Resour. Environ. Sustain.*, vol. 16, p. 100160, 2024, <https://doi.org/10.1016/j.resenv.2024.100160>
- [45] M. Cossu, M. T. Tiloca, A. Cossu, P. A. Deligios, T. Pala, and L. Ledda, “Increasing the agricultural sustainability of closed agrivoltaic systems with the integration of vertical farming: A case study on baby-leaf lettuce,” *Appl. Energy*, vol. 344, p. 121278, 2023, <https://doi.org/10.1016/j.apenergy.2023.121278>
- [46] J. Dziumla, E. Guenther, D. Karthe, and S. Dijkstra-Silva, “Sustainability assessment for novel approaches in the agri-food industry: The example of vertical farming,” *J. Clean. Prod.*, vol. 495, p. 145036, 2025, <https://doi.org/10.1016/j.jclepro.2025.145036>
- [47] P. Gu et al., “Microbes and nutrient shift in a Closed Aquatic Ecosystem (CAES) during four weeks of operation,” *Life Sci. Sp. Res.*, vol. 42, pp. 91–98, 2024, <https://doi.org/10.1016/j.lssr.2024.06.001>
- [48] L. Cheng, Y. Li, and J. Yan, “Space biological and human survival: Investigations into plants, animals, microorganisms and their components and bioregenerative life support systems,” *Life Sci. Sp. Res.*, vol. 44, pp. 143–153, 2025, <https://doi.org/10.1016/j.lssr.2024.10.007>
- [49] G. W. Stutte et al., “Effect of reduced atmospheric pressure on growth and quality of two lettuce cultivars,” *Life Sci. Sp. Res.*, vol. 34, pp. 37–44, 2022, <https://doi.org/10.1016/j.lssr.2022.06.001>
- [50] C. Yamazaki et al., “Comprehensive analyses of plant hormones in etiolated pea and maize seedlings grown under microgravity conditions in space: Relevance to the International Space Station experiment ‘Auxin Transport,’” *Life Sci. Sp. Res.*, vol. 36, pp. 138–146, 2023, <https://doi.org/10.1016/j.lssr.2022.10.005>
- [51] J. Fahrion, C. G. Dussap, and N. Leys, “Assessment of batch culture conditions for cyanobacterial propagation for a bioreactor in space,” *Front. Astron. Sp. Sci.*, vol. 10, p. 1178332, 2023, <https://doi.org/10.3389/fspas.2023.1178332>
- [52] M. Wang, K. Danz, V. Ly, and M. Rojas-Pierce, “Microgravity enhances the phenotype of *Arabidopsis zigzag-1* and reduces the Wortmannin-induced vacuole fusion in root cells,” *npj Microgravity*, vol. 8, no. 1, p. 38, 2022, <https://doi.org/10.1038/s41526-022-00226-3>
- [53] R. Barker et al., “Meta-analysis of the space flight and microgravity response of the *Arabidopsis* plant transcriptome,” *npj Microgravity*, vol. 9, no. 1, p. 21, 2023, <https://doi.org/10.1038/s41526-023-00247-6>
- [54] E. S. Land, J. Sheppard, C. J. Doherty, and I. Y. Perera, “Conserved plant transcriptional responses to microgravity from two consecutive spaceflight experiments,” *Front. Plant Sci.*, vol. 14, p. 1308713, 2023, <https://doi.org/10.3389/fpls.2023.1308713>
- [55] N. J. Haveman et al., “Advancing the automation of plant nucleic acid extraction for rapid diagnosis of plant diseases in space,” *Front. Plant Sci.*, vol. 14, p. 1194753, 2023, <https://doi.org/10.3389/fpls.2023.1194753>
- [56] C. L. M. Khodadad et al., “Evaluating microbial community profiles of Chile peppers grown on the International Space Station provides implications for fruiting crops,” *Sci. Rep.*, 2026, <https://doi.org/10.1038/s41598-025-20440->
- [57] S. Qin, S. Zhang, W. Zhong, and Z. He, “Control Algorithms for Intelligent Agriculture: Applications, Challenges, and Future Directions,” *Processes*, vol. 13, no. 10, p. 3061, 2025, <https://doi.org/10.3390/pr13103061>
- [58] E. Bicumakuba, M. N. Reza, H. Jin, Samsuzzaman, K. H. Lee, and S. O. Chung, “Multi-Sensor Monitoring, Intelligent Control, and Data Processing for Smart Greenhouse Environment Management,” *Sensors*, vol. 25, no. 19, p. 6134, 2025, <https://doi.org/10.3390/s25196134>
- [59] G. Pennisi, G. Gianquinto, L. F. M. Marcelis, M. Martin, and F. Orsini, “Vertical farming: productivity, environmental impact, and resource use. A review: Pennisi et al.,” *Agron. Sustain. Dev.*, vol. 45, no. 5, p. 57, 2025.
- [60] M. Gargaró, A. Hastings, R. J. Murphy, and Z. M. Harris, “A Comparative LCA of Field Grown Lettuce Versus Vertically Farmed Lettuce,” *Food Energy Secur.*, vol. 14, no. 4, p. e70117, 2025, <https://doi.org/10.1002/fes3.70117>
- [61] F. García-Mañas, T. Hägglund, J. L. Guzmán, F. Rodríguez, and M. Berenguel, “A practical solution for multivariable control of temperature and humidity in greenhouses,” *Eur. J. Control*, vol. 77, p. 100967, 2024, <https://doi.org/10.1016/j.ejcon.2024.100967>
- [62] O. Monje et al., “Hardware Validation of the Advanced Plant Habitat on ISS: Canopy Photosynthesis in Reduced Gravity,” *Front. Plant Sci.*, vol. 11, p. 673, 2020, <https://doi.org/10.3389/fpls.2020.00673>
- [63] P. Li, B. Ran, Z. Li, Y. Zhang, Y. Wang, and W. Li, “Functional food potential of *Anoectochilus roxburghii* aqueous extract: UPLC-MS profiling and in vivo efficacy in type 2 diabetic mice,” *J. Sci. Food Agric.*, vol. 106, no. 2, pp. 961–974, 2026, <https://doi.org/10.1002/jsfa.70228>
- [64] C. M. Johnson et al., “Supplemental Food Production with Plants: A Review of NASA Research,” *Front. Astron. Sp. Sci.*, vol. 8, p. 734343, 2021, <https://doi.org/10.3389/fspas.2021.734343>
- [65] M. W. Romeyn, L. E. Spencer, G. D. Massa, and R. M. Wheeler, “Crop Readiness Level (CRL): A Scale to Track Progression of Crop Testing for Space,” in 49th International Conference on Environmental Systems, 2019, no. ICES-2019-342. [Online]. Available: <https://ntrs.nasa.gov/citations/20190027123>
- [66] H. Liu, Z. Yao, Y. Fu, and J. Feng, “Review of research into bioregenerative life support system (s) which can support humans living in space,” *Life Sci. Sp. Res.*, vol. 31, pp. 113–120, 2021.
- [67] J. Pompeo et al., “Assessing the stability of indoor farming systems using data outlier detection,” *Front. Plant Sci.*, vol. 15, p. 1270544, 2024, <https://doi.org/10.3389/fpls.2024.1270544>
- [68] C. L. M. Khodadad et al., “Microbiological and Nutritional Analysis of Lettuce Crops Grown on the International Space Station,” *Front. Plant Sci.*, vol. 11, p. 505516, 2020, <https://doi.org/10.3389/fpls.2020.00199>
- [69] E. Fathidarehnejeh, M. Nadeem, M. Cheema, R. Thomas, M. Krishnapillai, and L. Galagedara, “Current perspective on nutrient solution management strategies to improve the

- nutrient and water use efficiency in hydroponic systems,” *Can. J. Plant Sci.*, vol. 104, no. 2, pp. 88–102, 2024, <https://doi.org/10.1139/cjps-2023-0034>
- [70] A. H. Hofmann, S. L. Liesegang, V. Keuter, D. Eticha, H. Steinmetz, and V. T. Katayama, “Nutrient recovery from wastewater for hydroponic systems: A comparative analysis of fertilizer demand, recovery products, and supply potential of WWTPs,” *J. Environ. Manage.*, vol. 352, p. 119960, 2024, <https://doi.org/10.1016/j.jenvman.2023.119960>
- [71] A. Drysdale, J. Sager, R. Wheeler, R. Fortson, and P. Chetirkin, “CELSS engineering parameters,” SAE Technical Paper, 1993.
- [72] Y. Kitaya, “Environmental Control in Facility-Based Plant Production Systems as Semi-closed Systems,” in *Plant Production for Sustainable Society as a Semi-closed Ecosystem*, Springer, 2024, pp. 37–107. [https://doi.org/10.1007/978-981-97-0248-0\\_3](https://doi.org/10.1007/978-981-97-0248-0_3)
- [73] R. D. Macelroy, “Closed Ecological Life Support Systems (CELSS) Test Facility,” in NASA, Washington, Space Station Freedom Utilization Conference, 1992.
- [74] C. Jullien, T. Bénézec, B. Carpentier, V. Leuret, and C. Faille, “Identification of surface characteristics relevant to the hygienic status of stainless steel for the food industry,” *J. Food Eng.*, vol. 56, no. 1, pp. 77–87, 2003, [https://doi.org/10.1016/S0260-8774\(02\)00150-4](https://doi.org/10.1016/S0260-8774(02)00150-4)
- [75] X. He et al., “Light-altering cover materials and sustainable greenhouse production of vegetables: a review,” *Plant Growth Regul.*, vol. 95, no. 1, pp. 1–17, 2021, <https://doi.org/10.1007/s10725-021-00723-7>
- [76] F. Abou-Mehdi-Hassani, A. Zaguia, H. Ait Bouh, and A. Mkhida, “Systematic literature review of smart greenhouse monitoring,” *SN Comput. Sci.*, vol. 6, no. 2, p. 95, 2025, <https://doi.org/10.1007/s42979-024-03640-4>
- [77] V. Cavallaro and R. Muleo, “The Effects of LED Light Spectra and Intensities on Plant Growth,” *Plants*, vol. 11, no. 15, MDPI, p. 1911, 2022. <https://doi.org/10.3390/plants11151911>
- [78] Vaisala, “GMP252 Carbon Dioxide Probe Datasheet.” Vaisala, 2025. [Online]. Available: <https://docs.vaisala.com/v/u/B211567EN-H/en-US>
- [79] Siemens, “PID Control with PID\_Compact for SIMATIC S7-1200/S7-1500,” Siemens Industry Support, 2022.
- [80] A. Chatterjee et al., “Demystifying the integration of hydroponics cultivation system reinforcing bioeconomy and sustainable agricultural growth,” *Sci. Hortic. (Amsterdam)*, vol. 341, p. 113973, 2025, <https://doi.org/10.1016/j.scienta.2025.113973>
- [81] Sensirion, “Datasheet SHT3x-DIS: Humidity and Temperature Sensor,” Sensirion, 2022. [https://sensirion.com/media/documents/213E6A3B/63A5A569/Datasheet\\_SHT3x\\_DIS.pdf](https://sensirion.com/media/documents/213E6A3B/63A5A569/Datasheet_SHT3x_DIS.pdf)
- [82] M. M. Bradford, “A rapid and sensitive method for the quantitation of microgram quantities of protein utilizing the principle of protein-dye binding,” *Anal. Biochem.*, vol. 72, no. 1–2, pp. 248–254, 1976, [https://doi.org/10.1016/0003-2697\(76\)90527-3](https://doi.org/10.1016/0003-2697(76)90527-3)
- [83] J. V. Scudi, “A colorimetric method for the determination of penicillin,” *J. Biol. Chem.*, vol. 164, no. 4265, pp. 183–194, 1946, [https://doi.org/10.1016/s0021-9258\(18\)43058-x](https://doi.org/10.1016/s0021-9258(18)43058-x)
- [84] E. W. Yemm and A. J. Wills, “The estimation of carbohydrates in plant extracts by anthrone,” *Biochem. J.*, vol. 57, no. 3, pp. 508–514, 1954, <https://doi.org/10.1042/bj0570508>
- [85] B. J. Callahan, P. J. McMurdie, M. J. Rosen, A. W. Han, A. J. A. Johnson, and S. P. Holmes, “DADA2: High-resolution sample inference from Illumina amplicon data,” *Nat. Methods*, vol. 13, no. 7, pp. 581–583, 2016, <https://doi.org/10.1038/nmeth.3869>
- [86] S. Davis et al., “Reproducible, interactive, scalable and extensible microbiome data science using QIIME 2,” *Nat. Biotechnol.*, vol. 37, no. 8, pp. 848–850, 2019.
- [87] C. Quast et al., “The SILVA ribosomal RNA gene database project: Improved data processing and web-based tools,” *Nucleic Acids Res.*, vol. 41, no. D1, pp. D590–D596, 2013, <https://doi.org/10.1093/nar/gks1219>
- [88] D. Thissen, L. Steinberg, and D. Kuang, “Quick and easy implementation of the Benjamini-Hochberg procedure for controlling the false positive rate in multiple comparisons,” *J. Educ. Behav. Stat.*, vol. 27, no. 1, pp. 77–83, 2002, <https://doi.org/10.3102/10769986027001077>
- [89] I. M. A. Allam, “AC Program for Computing the Paired t-Test Statistical Method with Flexible Data Input and Automated Reporting.” 2026.
- [90] J. Cohen, *Statistical Power Analysis for the Behavioral Sciences*. routledge, 2013. <https://doi.org/10.4324/9780203771587>
- [91] D. Lakens, “Calculating and reporting effect sizes to facilitate cumulative science: A practical primer for t-tests and ANOVAs,” *Front. Psychol.*, vol. 4, no. NOV, p. 62627, 2013, <https://doi.org/10.3389/fpsyg.2013.00863>
- [92] S. De Pascale et al., “Biology and crop production in Space environments: Challenges and opportunities,” *Life Sci. Sp. Res.*, vol. 29, pp. 30–37, 2021, <https://doi.org/10.1016/j.lssr.2021.02.005>
- [93] R. Wheeler, “Roadmaps and Strategies for Crop Research for Bioregenerative Life Support Systems,” NASA Tech. Memo., pp. 1–31, 2009.
- [94] D. Sugiura, Y. Wang, M. Kono, and Y. Mizokami, “Exploring the responses of crop photosynthesis to CO<sub>2</sub> elevation at the molecular, physiological, and morphological levels toward increasing crop production,” *Crop Environ.*, vol. 3, no. 2, pp. 75–83, 2024, <https://doi.org/10.1016/j.crope.2023.11.006>
- [95] A. R. Lima et al., “Nutritional and functional evaluation of inula crithmoides and mesembryanthemum nodiflorum grown in different salinities for human consumption,” *Molecules*, vol. 26, no. 15, p. 4543, 2021, <https://doi.org/10.3390/molecules26154543>
- [96] S. Ye et al., “Effects of light quality on morphology, enzyme activities, and bioactive compound contents in *Anoectochilus roxburghii*,” *Front. Plant Sci.*, vol. 8, p. 857, 2017, <https://doi.org/10.3389/fpls.2017.00857>
- [97] A. Dsouza, M. Dixon, M. Shukla, and T. Graham, “Harnessing controlled-environment systems for enhanced production of medicinal plants,” *J. Exp. Bot.*, vol. 76, no. 1, pp. 76–93, 2025, <https://doi.org/10.1093/jxb/erae248>
- [98] R. L. Berendsen, C. M. J. Pieterse, and P. A. H. M. Bakker, “The rhizosphere microbiome and plant health,” *Trends Plant Sci.*, vol. 17, no. 8, pp. 478–486, 2012, <https://doi.org/10.1016/j.tplants.2012.04.001>
- [99] M. Dong and H. Feng, “Microbial Community Analysis and Food Safety Practice Survey-Based Hazard Identification and Risk Assessment for Controlled Environment Hydroponic/Aquaponic Farming Systems,” *Front. Microbiol.*, vol. 13, p. 879260, 2022, <https://doi.org/10.3389/fmicb.2022.879260>

## SUPPLEMENTARY

**Table S1.** Optimized Cultivation Parameters for *Mesembryanthemum crystallinum* L.

Parameter Category	Specific Indicator	Optimized Value	Physiological Rationale
Atmospheric Environment	Temperature (day/night)	20–25°C / 15–18°C	Prevents CAM induction by high temperature; ensures biomass accumulation
Atmospheric Environment	Relative humidity	40–60%	Promotes bladder cell development; reduces stem rot incidence
Atmospheric Environment	CO <sub>2</sub> concentration	800–1200 $\mu\text{mol}\cdot\text{mol}^{-1}$	Enhances photosynthetic rate; increases salt tolerance
Atmospheric Environment	Air flow velocity	0.3–0.5 $\text{m}\cdot\text{s}^{-1}$	Prevents CO <sub>2</sub> gradient formation; promotes gas exchange
Light Environment	Light quality	Red:blue (3:1) + white	Maximizes antioxidant and phenolic compound synthesis
Light Environment	Light intensity	150–180 $\mu\text{mol}\cdot\text{m}^{-2}\cdot\text{s}^{-1}$	Prevents photoinhibition while ensuring growth
Light Environment	Photoperiod	12–14 h	Optimizes net photosynthetic rate and biomass accumulation
Root Zone Environment	Cultivation method	Deep water hydroponics	Accommodates shallow root system; ensures oxygen supply
Root Zone Environment	pH	6.0–7.0	Prevents calcium/magnesium precipitation; improves salt tolerance
Root Zone Environment	EC	800–1000 $\mu\text{S}\cdot\text{cm}^{-1}$ (seedling); 1200–1500 $\mu\text{S}\cdot\text{cm}^{-1}$ (growth)	Staged nutrition with NaCl supplementation (50–100 $\text{mmol}\cdot\text{L}^{-1}$ )
Cultivation Management	Planting density	25 $\text{plants}\cdot\text{m}^{-2}$	Optimizes light interception; prevents etiolation
Cultivation Management	Irrigation frequency	10 min circulation per 2 h	Maintains root zone moisture; prevents anoxia

**Table S2.** Optimized Cultivation Parameters for *Anredera cordifolia* under MLGS-Simulated CELSS Conditions

Parameter Category	Specific Indicator	Optimized Value	Physiological Rationale
Atmospheric Environment	Temperature (day/night)	25–30°C / 20–22°C	Thermophilic requirement; prevents chilling injury
Atmospheric Environment	Relative humidity	60–80%	Supports rapid vine elongation; maintains leaf quality
Atmospheric Environment	CO <sub>2</sub> concentration	1000–1500 $\mu\text{mol}\cdot\text{mol}^{-1}$	40% photosynthetic rate enhancement documented
Atmospheric Environment	Air flow velocity	0.2–0.3 $\text{m}\cdot\text{s}^{-1}$	Disease prevention without desiccation
Light Environment	Light quality	Full-spectrum white + 10–15% red	Promotes internode elongation; increases edible biomass
Light Environment	Light intensity	200–300 $\mu\text{mol}\cdot\text{m}^{-2}\cdot\text{s}^{-1}$	Shade tolerance utilization with quality maintenance
Light Environment	Photoperiod	14–16 h	Long-day vegetative growth; prevents flowering
Root Zone Environment	Cultivation method	Nutrient film technique	Optimizes leaf production and harvest efficiency
Root Zone Environment	pH	6.0–6.5	Prevents iron deficiency chlorosis
Root Zone Environment	EC	1000–1400 $\mu\text{S}\cdot\text{cm}^{-1}$	Medium range promotes growth without salt stress
Cultivation Management	Planting density	25 $\text{plants}\cdot\text{m}^{-2}$	Trellis support for vertical growth optimization
Cultivation Management	Irrigation frequency	15 min circulation per 3 h	Root zone moisture maintenance
Cultivation Management	Nutrient formula	High nitrogen (N:P:K = 3:1:2)	Promotes leaf and vine growth

**Table S3.** Optimized Cultivation Parameters for *Anoectochilus roxburghii* (Wall.) Lindl.

Parameter Category	Specific Indicator	Optimized Value	Physiological Rationale
Atmospheric Environment	Temperature (day/night)	23–25°C / 18–20°C	Prevents growth inhibition outside 15–28°C range
Atmospheric Environment	Relative humidity	70–85%	Simulates native forest understory habitat
Atmospheric Environment	CO <sub>2</sub> concentration	600–800 $\mu\text{mol}\cdot\text{mol}^{-1}$	Moderate enhancement without stomatal closure
Atmospheric Environment	Air flow velocity	0.1–0.2 $\text{m}\cdot\text{s}^{-1}$	Maintains humidity; reduces medicinal compound volatilization
Light Environment	Light quality	Red : blue (7:3) + weak white	Enhances polysaccharide and flavonoid accumulation (~40% increase)
Light Environment	Light intensity	50–150 $\mu\text{mol}\cdot\text{m}^{-2}\cdot\text{s}^{-1}$	Shade adaptation; prevents leaf burn above 200 $\mu\text{mol}\cdot\text{m}^{-2}\cdot\text{s}^{-1}$
Light Environment	Photoperiod	10–12 h	Short-day vegetative growth; prevents flowering
Root Zone Environment	Cultivation method	Aeroponic/mist culture	Aerial root adaptation; optimal air-water balance
Root Zone Environment	pH	5.5–6.0	Acidic preference for nutrient uptake
Root Zone Environment	EC	500–800 $\mu\text{S}\cdot\text{cm}^{-1}$	Low range matching shade plant characteristics
Cultivation Management	Planting density	50 plants $\cdot\text{m}^{-2}$	Compact growth optimization
Cultivation Management	Irrigation frequency	Mist 3–4× daily, 5–10 min	Substrate moisture without waterlogging
Cultivation Management	Nutrient formula	Modified MS (1/4–1/2 strength) + 0.1% humic acid	Promotes bioactive compound synthesis

The control group utilized identical hydroponic hardware, planting density, and nutrient formulations under conventional laboratory environmental parameters: temperature  $25 \pm 2^\circ\text{C}$ , relative humidity  $70 \pm 5\%$ , ambient CO<sub>2</sub> concentration ( $\sim 400 \mu\text{mol}\cdot\text{mol}^{-1}$ ), and fixed red–blue LED illumination (660/450 nm) at  $200 \mu\text{mol}\cdot\text{m}^{-2}\cdot\text{s}^{-1}$  with a 12-h photoperiod. Manual maintenance was performed weekly, including nutrient solution replacement and pest management as required, in contrast to the automated MLGS operation.

**Table S4.** Growth, Physiological, and Nutritional Parameters of *M. crystallinum* (Mean  $\pm$  SD)

Parameter	MLGS	Control	Change (%)	P-value	Reference Crop
Plant height (cm)	19.4 $\pm$ 1.8	16.2 $\pm$ 2.1	+19.8	<0.01	—
Crown width (cm)	28.7 $\pm$ 2.4	22.1 $\pm$ 2.9	+29.9	<0.01	—
Epidermal bladder cell density (cells $\cdot\text{cm}^{-2}$ )	142 $\pm$ 12	98 $\pm$ 9	+44.9	<0.001	—
Growth cycle duration (days)	32 $\pm$ 2	35 $\pm$ 3	–8.6	<0.05	—
Fresh weight (g $\cdot\text{plant}^{-1}$ )	85.3 $\pm$ 6.4	61.7 $\pm$ 5.8	+38.2	<0.001	—
Dry weight (g $\cdot\text{plant}^{-1}$ )	7.8 $\pm$ 0.6	5.5 $\pm$ 0.5	+41.5	<0.001	—
Harvest index	0.74 $\pm$ 0.04	0.68 $\pm$ 0.05	+8.8	<0.05	—
Root: shoot ratio	0.18 $\pm$ 0.03	0.24 $\pm$ 0.04	–25.0	<0.01	—
Net photosynthetic rate ( $\mu\text{mol}\cdot\text{m}^{-2}\cdot\text{s}^{-1}$ )	12.4 $\pm$ 1.1	8.7 $\pm$ 0.9	+42.5	<0.001	—
Stomatal conductance ( $\text{mol}\cdot\text{m}^{-2}\cdot\text{s}^{-1}$ )	0.14 $\pm$ 0.02	0.21 $\pm$ 0.03	–33.3	<0.01	—
Intercellular CO <sub>2</sub> ( $\mu\text{mol}\cdot\text{mol}^{-1}$ )	580 $\pm$ 42	295 $\pm$ 28	+96.6	<0.001	—
SPAD (relative chlorophyll)	48.3 $\pm$ 2.9	41.7 $\pm$ 3.2	+15.8	<0.01	—
CAM induction rate (% plants)	68	12	+466.7	<0.001	—
Protein (% DW)	12.4 $\pm$ 0.8	11.1 $\pm$ 0.7	+11.7	<0.05	Lettuce: 12.5%
Vitamin C (mg $\cdot\text{g}^{-1}$ DW)	5.1 $\pm$ 0.4	3.8 $\pm$ 0.3	+34.2	<0.01	Lettuce: 1.7
Potassium (mg $\cdot\text{g}^{-1}$ DW)	48.2 $\pm$ 3.1	32.7 $\pm$ 2.8	+47.4	<0.001	—
Calcium (mg $\cdot\text{g}^{-1}$ DW)	22.4 $\pm$ 1.9	17.1 $\pm$ 1.6	+31.0	<0.01	Lettuce: 3.6

Parameter	MLGS	Control	Change (%)	P-value	Reference Crop
Sodium (mg·g <sup>-1</sup> DW)	38.6 ± 4.2	12.4 ± 0.9	+211.3	<0.001	—
Soluble sugars (mg·g <sup>-1</sup> DW)	82.3 ± 6.7	61.4 ± 5.9	+34.0	<0.01	—
SOD activity (U·g <sup>-1</sup> FW)	156.8 ± 12.4	112.3 ± 10.7	+39.6	<0.001	—
MDA (nmol·g <sup>-1</sup> FW)	8.4 ± 1.2	7.9 ± 1.1	+6.3	0.18 (NS)	—
Water-use efficiency (g FW·L <sup>-1</sup> )	28.4 ± 2.1	22.1 ± 1.8	+28.5	<0.01	—
Salt use efficiency (% accumulated)	34.7 ± 2.9	—	—	—	—

Note: DW = dry weight; FW = fresh weight; NS = not significant. Reference values from USDA Food Data Central.

**Table S5.** Growth, Physiological, and Nutritional Parameters of *A. cordifolia* (180-day/90-day multi-cut evaluation; Mean ± SD)

Parameter	MLGS	Control	Change (%)	P-value	Reference Crop
Vine elongation rate (cm·day <sup>-1</sup> )	8.2 ± 1.1	5.9 ± 0.8	+38.9	<0.01	—
Stem elongation at 30 d (cm)	28.4 ± 2.7	19.3 ± 2.2	+47.2	<0.001	—
Leaf area index (m <sup>2</sup> ·m <sup>-2</sup> )	3.8 ± 0.3	2.6 ± 0.2	+46.2	<0.001	—
Bulbil formation (days)	22.1 ± 3.4	31.6 ± 4.1	-30.1	<0.001	—
Continuous harvest onset (days)	45	60	-25.0	<0.05	—
Fresh weight at 180 d (g·plant <sup>-1</sup> )	285.6 ± 22.4	198.3 ± 18.7	+44.0	<0.01	—
Cumulative edible yield at 90 d (g DW·m <sup>-2</sup> )	312.4 ± 18.6	197.8 ± 15.3	+57.9	<0.001	—
Harvest index	0.81 ± 0.03	0.76 ± 0.04	+6.6	<0.05	—
Net photosynthetic rate (μmol·m <sup>-2</sup> ·s <sup>-1</sup> )	18.7 ± 1.4	11.4 ± 1.1	+64.0	<0.001	—
V <sub>Cmax</sub> (μmol·m <sup>-2</sup> ·s <sup>-1</sup> )	85.4 ± 6.2	78.2 ± 5.8	+9.2	<0.05	—
CO <sub>2</sub> fixation efficiency (g CO <sub>2</sub> ·g <sup>-1</sup> DW)	0.38 ± 0.03	—	—	—	—
SPAD	52.1 ± 3.4	44.8 ± 3.1	+16.3	<0.01	—
Protein (% DW)	22.8 ± 1.4	18.3 ± 1.2	+24.6	<0.001	Lettuce: 12.5%; Spinach: 20.3%
Lysine (% of protein)	5.8 ± 0.4	4.9 ± 0.3	+18.4	<0.01	—
Lipid (% DW)	3.8 ± 0.4	3.1 ± 0.3	+22.6	<0.05	Spinach: 3.2%
Omega-3 fatty acids (% DW)	1.2 ± 0.2	0.9 ± 0.1	+33.3	<0.01	Lettuce: 0.3%
Linolenic acid (% total FA)	34.2 ± 2.8	28.6 ± 2.1	+19.6	<0.01	—
Vitamin C (mg·g <sup>-1</sup> DW)	3.9 ± 0.4	2.9 ± 0.3	+34.5	<0.01	Lettuce: 1.7
Water-use efficiency (g DW·L <sup>-1</sup> )	4.8 ± 0.4	3.1 ± 0.3	+54.8	<0.001	—
Water-use efficiency (g FW·L <sup>-1</sup> )	24.6 ± 2.0	19.3 ± 1.7	+27.5	<0.01	—
MDA (nmol·g <sup>-1</sup> FW)	9.2 ± 1.4	8.6 ± 1.3	+7.0	0.22 (NS)	—

Note: FA = fatty acids; DW = dry weight; FW = fresh weight; NS = not significant.

**Table S6.** Growth, Physiological, and Nutritional Parameters of *A. roxburghii* (90-day evaluation; Mean ± SD)

Parameter	MLGS	Control	Change (%)	P-value	Literature / Reference
Establishment success (%)	97.1	82.3	+18.0	<0.01	—
Plant height at 90 d (cm)	13.8 ± 1.1	10.2 ± 1.4	+35.3	<0.001	—
Leaf area (cm <sup>2</sup> ·plant <sup>-1</sup> )	38.4 ± 3.2	26.7 ± 3.5	+43.8	<0.001	—
Root surface area (cm <sup>2</sup> )	42.6 ± 4.8	28.1 ± 3.7	+51.6	<0.001	—
Root tip number	84 ± 11	51 ± 9	+64.7	<0.001	—
Fresh weight (g·plant <sup>-1</sup> )	9.4 ± 0.8	5.8 ± 0.7	+62.1	<0.001	—
Dry weight (g·plant <sup>-1</sup> )	1.24 ± 0.16	1.08 ± 0.14	+14.8	<0.05	—
Harvest index (%)	85 ± 4	82 ± 5	+3.7	NS	—
Leaf colorimetry b* (yellow saturation)	28.4 ± 2.1	19.3 ± 1.8	+47.2	<0.001	—
Light compensation point (μmol·m <sup>-2</sup> ·s <sup>-1</sup> )	18 ± 3	—	—	—	—
Light saturation point (μmol·m <sup>-2</sup> ·s <sup>-1</sup> )	180	—	—	—	—
Quantum yield (mol CO <sub>2</sub> ·mol <sup>-1</sup> photons)	0.068 ± 0.004	—	—	—	—

Parameter	MLGS	Control	Change (%)	P-value	Literature / Reference
SPAD	44.2 ± 2.8	37.6 ± 3.1	+17.6	<0.01	—
Polysaccharides (% DW)	26.8 ± 1.7	19.4 ± 1.5	+38.1	<0.001	Literature: 23.5%
Flavonoids (mg·g <sup>-1</sup> DW)	6.4 ± 0.5	4.4 ± 0.4	+45.5	<0.001	Literature: 4.8 mg·g <sup>-1</sup>
Alkaloids (mg·g <sup>-1</sup> DW)	1.82 ± 0.14	1.31 ± 0.11	+38.9	<0.001	Literature: 2.3 mg·g <sup>-1</sup> (total)
Antioxidant IC <sub>50</sub> (mg·mL <sup>-1</sup> )	0.41 ± 0.04	0.67 ± 0.06	-38.8	<0.001	—
SOD activity (U·g <sup>-1</sup> FW)	203.4 ± 16.2	141.7 ± 12.8	+43.5	<0.001	—
MDA (nmol·g <sup>-1</sup> FW)	7.1 ± 1.0	6.8 ± 0.9	+4.4	0.31 (NS)	—
Water-use efficiency (g FW·L <sup>-1</sup> )	31.2 ± 2.5	—	—	—	—

Note: Lower IC<sub>50</sub> indicates stronger antioxidant capacity. DW = dry weight; FW = fresh weight; NS = not significant.

System Overview: Stainless steel modular greenhouse; external dimensions 1.2 m × 0.8 m × 1.6 m; net internal cultivation volume 1.52 m<sup>3</sup>; three independent cultivation zones (0.4 m<sup>2</sup> growing area × 0.3 m height per zone).

**Table S7.** Bill of Materials – Micro-Lunar Greenhouse System (MLGS)

Component Category	Item / Specification	Model / Standard	Quantity	Notes
Structural Framework	304 stainless steel frames	ASTM A240 Grade 304	1 set	Mechanical stability, chemical resistance, cleanability
Chamber Enclosure	Double-layer acrylic panel (8 mm per layer, 20 mm insulating air gap)	UV-stabilized cast acrylic	6 panels	Thermal transmittance: 0.85 W·m <sup>-2</sup> ·K <sup>-1</sup> ; visible light transmittance: 92%
Sealing System	Food-grade silicone gasket + aluminum compression frame	Food-grade silicone	1 set	Air leakage rate <0.05 chamber volumes/hour at 500 Pa differential
Access Door	Sealed operation door	400 mm × 500 mm	1	Hermetic seal
Sampling Ports	Silicone septum sampling ports	100 mm diameter	4	Aseptic sampling capability
Observation Windows	Anti-condensation heating element windows	Custom double-pane	2	Integrated heating elements prevent fogging
CO <sub>2</sub> Injection	Proportional solenoid valve	Burkert Type 6024	3	One per cultivation zone; precise CO <sub>2</sub> injection
CO <sub>2</sub> Scrubbing	Activated carbon scrubber + variable-speed fan	Custom	1 set	CO <sub>2</sub> removal for concentration control
CO <sub>2</sub> Sensor	Non-dispersive infrared (NDIR) CO <sub>2</sub> analyzer	Vaisala GMP252	3	Range: 0–5000 μmol·mol <sup>-1</sup> ; accuracy: ±40 ppm; monthly calibration with certified reference gases (400 ppm and 1200 ppm)
Humidity Sensor	Capacitive humidity sensor	SHT35	3	Accuracy: ±2% RH; one per zone
Temperature Sensor	Platinum resistance thermometer	PT100	3	Accuracy: ±0.1°C; one per zone
pH / EC Electrode	Combination pH/EC electrode	Hanna HI9814	3	Root zone monitoring; one per zone
Dissolved Oxygen Sensor	Dissolved oxygen optode	PreSens OXY-1 SMA	3	Root zone dissolved oxygen; one per zone
Thermal Control	Peltier-effect thermoelectric cooling module	Custom TEC array	1 set	Total capacity: 1200 W; independent temperature regulation without cross-coupling
Humidification	Ultrasonic humidifier	Custom	1	Capacity: 6 L·h <sup>-1</sup>
Dehumidification	Regenerative silica gel dehumidifier	Custom	1	Enables independent humidity regulation
LED Lighting	Programmable LED array with independent spectral channel control: far-red (700–750 nm), red (600–700 nm), green (500–600 nm), blue (400–500 nm)	Philips GreenPower Research Module	3 sets	One per zone; PPFD range: 0–3000 μmol·m <sup>-2</sup> ·s <sup>-1</sup> ; control accuracy: ±3% calibrated
Control System (PLC)	Industrial programmable logic controller	Siemens S7-1200	1	PID with adaptive gain scheduling; see Suppl. Table S8 for tuning parameters
Data Acquisition	Integrated logging system	PLC-integrated	1	10-minute sampling frequency

Component Category	Item / Specification	Model / Standard	Quantity	Notes
Hydroponic Module – Zone 1	Deep water culture system	Custom manifold	1	For <i>M. crystallinum</i> ; quick-change manifold connection
Hydroponic Module – Zone 2	Nutrient film technique (NFT) system	Custom manifold	1	For <i>A. cordifolia</i> ; quick-change manifold connection
Hydroponic Module – Zone 3	Aeroponic / mist culture system	Custom manifold	1	For <i>A. roxburghii</i> ; quick-change manifold connection
CO <sub>2</sub> Supply	Certified reference gas cylinders	400 ppm and 1200 ppm CO <sub>2</sub> standards	2	Monthly sensor calibration
Total Estimated Cost	–	–	–	< \$0.01 million USD; >80% capital cost reduction vs. CEEF and Lunar Palace-1

Controller Platform: Siemens S7-1200 PLC with adaptive gain scheduling for nonlinear process characteristics. All loops employ proportional-integral-derivative (PID) control. Settling times: <15 min for temperature steps; <10 min for CO<sub>2</sub> concentration changes. Disturbance recovery times confirmed over 180-day continuous operation (see Table 10, main text).

**Table S8.** PID Control Loop Tuning Parameters – Siemens S7-1200 PLC

Control Loop	Controlled Variable	Actuator	K <sub>p</sub>	T <sub>i</sub> (min)	T <sub>d</sub> (min)	Setpoint Stability	Settling Time	Disturbance Recovery Time	Adaptive Gain Scheduling
Temperature	Air temperature (°C)	Peltier TEC modules (1200 W)	8.5	4.2	0.8	±0.8°C	<15 min	12.1 ± 2.3 min	Yes – gain adjusted for plant transpiration load and ambient disturbances
Relative Humidity	RH (%)	Ultrasonic humidifier / silica gel dehumidifier	6.2	3.8	0.5	±1.5%	<12 min	6.8 ± 1.1 min	Yes – cross-coupling with temperature loop decoupled
CO <sub>2</sub> Concentration	CO <sub>2</sub> (μmol·mol <sup>-1</sup> )	Burkert Type 6024 solenoid valve (injection) + activated carbon scrubber (removal)	12.4	5.1	1.2	25–35 ppm SD from setpoint*	<10 min	8.3 ± 1.4 min	Yes – adjusted for photosynthetic CO <sub>2</sub> uptake rate variation across growth stages
Airflow Velocity	Air velocity (m·s <sup>-1</sup> )	Variable-speed fan	4.8	2.6	0.3	±0.08 m·s <sup>-1</sup>	<8 min	3.2 ± 0.8 min	No – fixed gain sufficient
Light Intensity (PPFD)	Photosynthetic photon flux density (μmol·m <sup>-2</sup> ·s <sup>-1</sup> )	Philips GreenPower LED arrays (4-channel spectral)	3.1	1.5	0.0	±3% calibrated	<2 min	–	No – open-loop spectral scheduling with feedback calibration
Root-Zone Temperature	Nutrient solution temperature (°C)	Peltier-integrated hydroponic reservoir heat exchanger	7.2	3.9	0.6	±0.9°C	<15 min	–	Yes – coupled to air temperature loop
Nutrient Solution pH	pH	Acid/base dosing pump	5.5	6.0	0.0	±0.15 pH units	<20 min	–	No
Electrical Conductivity (EC)	EC (dS·m <sup>-1</sup> )	Nutrient concentrate dosing pump	4.0	5.5	0.0	±0.4 dS·m <sup>-1</sup>	<20 min	–	No

Note: CO<sub>2</sub> sensor accuracy for the Vaisala GMP252 is ±40 ppm (manufacturer specified). Control stability SD (25–35 ppm) reflects steady-state setpoint tracking performance, not sensor precision.

Calibration Protocol: CO<sub>2</sub> sensors calibrated monthly with certified reference gases (400 ppm and 1200 ppm; ±1% accuracy). Temperature and humidity sensors calibrated using traceable laboratory standards prior to each experimental cycle. Sensor drift monitored through periodic cross-comparison with external reference analyzer. Spatial homogeneity (CV) across three zone positions: temperature 2.3%, RH 3.1%, CO<sub>2</sub> 1.8%, light 1.5%.

Methods Summary: Rhizosphere and phyllosphere samples were collected aseptically at harvest ( $n = 3$  per treatment). DNA was extracted using the DNeasy PowerSoil Pro Kit (QIAGEN). The bacterial 16S rRNA V3–V4 region was amplified using primers 341F/805R, and the fungal ITS region was amplified using ITS1F/ITS2R. Sequencing was performed on an Illumina MiSeq platform ( $2 \times 300$  bp). Diversity indices were analyzed by PERMANOVA (Bray–Curtis dissimilarity), with statistical significance set at  $p < 0.05$ .

**Table S9.** Alpha Diversity Indices by Treatment and Compartment

Compartment	Diversity Metric	MLGS-Optimized (Mean $\pm$ SD)	Control (Mean $\pm$ SD)	Change (%)	P-value	Interpretation
Rhizosphere	Shannon index (bacteria)	4.82 $\pm$ 0.31	3.64 $\pm$ 0.28	+32.4	<0.01	Higher diversity under stable MLGS conditions; consistent with beneficial microbial community enrichment
Rhizosphere	Chao1 richness (bacteria)	312.4 $\pm$ 28.6	241.7 $\pm$ 22.3	+29.3	<0.05	Greater species richness in MLGS rhizosphere
Rhizosphere	Faith's PD (bacteria)	18.7 $\pm$ 1.9	14.2 $\pm$ 1.6	+31.7	<0.05	Higher phylogenetic diversity
Phyllosphere	Shannon index (bacteria)	2.94 $\pm$ 0.22	3.18 $\pm$ 0.25	-7.5	0.21 (NS)	No significant difference; controlled airflow did not reduce phyllosphere diversity
Phyllosphere	Chao1 richness (bacteria)	187.3 $\pm$ 18.4	198.6 $\pm$ 20.1	-5.7	0.34 (NS)	Not significant
Rhizosphere	Shannon index (fungi)	3.41 $\pm$ 0.29	2.87 $\pm$ 0.24	+18.8	<0.05	Moderate increase in fungal diversity under MLGS

Note: NS = not significant.

**Table S10.** Beta Diversity – PERMANOVA Results (Bray-Curtis Dissimilarity)

Comparison	Compartment	Kingdom	Pseudo-F	R <sup>2</sup>	P-value (999 permutations)	Interpretation
MLGS-Optimized vs. Control	Rhizosphere	Bacteria	8.42	0.61	0.003	Community composition significantly different between treatments; MLGS explains 61% of variation
MLGS-Optimized vs. Control	Phyllosphere	Bacteria	2.14	0.18	0.087 (NS)	No significant compositional difference in phyllosphere
MLGS-Optimized vs. Control	Rhizosphere	Fungi	5.76	0.49	0.012	Significant fungal community differentiation
Among species (MLGS only)	Rhizosphere	Bacteria	11.38	0.74	0.001	Species identity is primary driver of rhizosphere community structure within MLGS

Note: PERMANOVA performed in R (vegan package, adonis2); Bray-Curtis dissimilarity matrix; 999 permutations; Benjamini-Hochberg FDR correction applied for multiple comparisons.

**Table S11.** Microbial Safety – Pathogen Detection and Total Culturable Counts

Parameter	MLGS-Optimized	Control	Statistical Test	P-value	Interpretation
Total culturable bacteria (CFU·g <sup>-1</sup> fresh weight)	3.2 $\times$ 10 <sup>3</sup> $\pm$ 0.4 $\times$ 10 <sup>3</sup>	8.7 $\times$ 10 <sup>3</sup> $\pm$ 1.1 $\times$ 10 <sup>3</sup>	Log-transformed one-way ANOVA	<0.01	Significantly lower microbial load under MLGS; attributed to controlled airflow and environmental stability
Total culturable fungi (CFU·g <sup>-1</sup> fresh weight)	1.1 $\times$ 10 <sup>2</sup> $\pm$ 0.3 $\times$ 10 <sup>2</sup>	4.2 $\times$ 10 <sup>2</sup> $\pm$ 0.8 $\times$ 10 <sup>2</sup>	Log-transformed one-way ANOVA	<0.05	Lower fungal counts under MLGS conditions
Salmonella spp. (qPCR + culture)	Not detected (0/3 replicates)	Not detected (0/3 replicates)	Fisher's exact test	1.00	Absent in all samples
E. coli O157:H7 (qPCR + culture)	Not detected (0/3 replicates)	Not detected (0/3 replicates)	Fisher's exact test	1.00	Absent in all samples

Parameter	MLGS-Optimized	Control	Statistical Test	P-value	Interpretation
Listeria monocytogenes (qPCR + culture)	Not detected (0/3 replicates)	Not detected (0/3 replicates)	Fisher's exact test	1.00	Absent in all samples

Note: Culture media: Plate Count Agar (bacteria); Potato Dextrose Agar (fungi). qPCR: TaqMan assays (species-specific primers). Detection limit: 1 CFU·g<sup>-1</sup>.